SENSING APPLICATIONS OF FLUCTUATIONS AND NOISE

A Dissertation

by

HUNG-CHIH CHANG

Submitted to the Office of Graduate Studies of
Texas A&M University
in partial fulfillment of the requirements for the degree of

DOCTOR OF PHILOSOPHY

December 2010

Major Subject: Electrical Engineering

SENSING APPLICATIONS OF FLUCTUATIONS AND NOISE

A Dissertation

by

HUNG-CHIH CHANG

Submitted to the Office of Graduate Studies of
Texas A&M University
in partial fulfillment of the requirements for the degree of

DOCTOR OF PHILOSOPHY

Approved by:

Chair of Committee,	Laszlo B. Kish
Committee Members,	Charles T. Hallmark
	Arum Han
	Jun Kameoka
Head of Department,	Costas N. Georghiades

December 2010

Major Subject: Electrical Engineering

ABSTRACT

Sensing Applications of Fluctuations and Noise.

(December 2010)

Hung-Chih Chang, B.S., National Central University, Taoyuan, Taiwan;

M.S., National Chiao Tung University, Hsinchu, Taiwan

Chair of Advisory Committee: Dr. Laszlo Kish

Noise and time-dependent fluctuations are usually undesirable signals. However, they have many applications. This dissertation deals with two kinds of sensing applications of fluctuation and noise: soil bulk density assessment and bacterium sensing.

The measurement of Vibration-Induced Conductivity Fluctuations (VICOF) provides information about the bulk density and other parameters of soils. Bulk density is the physical property of soils that is important to both the agriculture and construction industries. The traditional measurements of soil bulk density are often time-consuming, expensive or destructive. To determine the soil bulk density without the above drawbacks, the VICOF measurement scheme was proposed. The research of VICOF in this dissertation includes two parts: the initial phase of study and the new methods and their theory. In the initial phase of study, the simple experiments, theory, and simulations of VICOF were tested for relations between the soil bulk density, wetness, salinity, and the VICOF data. Then, new measurement arrangements and their theoretical models were proposed to improve the weaknesses of the initial approach (such as large

scattering of data due to loose and heavy contacts) and to calculate the relationship between the measured signals and the electromechanical transport parameters of the soils.

The bacterium sensing study in this dissertation was proposed to explore simple, practical, rapid, sensitive, specific, portable, and inexpensive ways to detect and recognize bacteria by Fluctuation-Enhanced Sensing (FES). One such potential way of bacterium sensing is to analyze their odor. The research of bacterium sensing also includes two parts: the initial phase of study and the new methods and their theory. The initial phase study was proposed to explore the possibility of detecting and identifying bacteria by sensing their odor via FES with commercial Taguchi sensors. Then the subsequently developed new methods and their theory provide a simple way to generate binary patterns with perfect reproducibility based on the spectral slopes in different frequency ranges at FES. This new type of signal processing and pattern recognition is implemented at the block diagram level using the building elements of analog circuitries and a few logic gates with total power consumption in the microWatts range.

To My Family, Chuen Chang, Ching-Ning Lai and Tzu-Fen Chang

ACKNOWLEDGEMENTS

I would like to thank my committee chair, Dr. Kish, my committee members, Dr. Kameoka, Dr. Han, and Dr. Hallmark, and co-researcher: Dr. Maria D. King, Dr. Zoltan Gingl, and Dr. Chiman Kwan for their guidance and support throughout the course of this research.

Thanks also go to my friends, colleagues, the department faculty and staff for making my time at Texas A&M University a great experience. I also want to extend my gratitude to the University Writing Center, which provided the writing consultation service.

Finally, thanks to my father, mother, and sister for their encouragement and love.

NOMENCLATURE

VICOF	Vibration-Induced Conductivity Fluctuation
FES	Fluctuation-Enhanced Sensing
ECa	Apparent Electrical Conductivity
TDR	Time-Domain Reflectometry
DC	Direct Current
AC	Alternating Current
EN	Electronic Nose
ET	Electronic Tongue
DSP	Digital Signal Processor
TSA	Tryptic Soy Agar
E. coli	Escherichia Coli
Anthrax	Anthrax Surrogate *Bacillus Subtilis*

TABLE OF CONTENTS

Page

LIST OF FIGURES

Page

Page

Page

LIST OF TABLES

1. INTRODUCTION*

Noise and fluctuations are usually undesirable signals disturbing the accuracy of information and are ubiquitous in life. Everywhere, people who try to deal with signals need to overcome the background noise by arriving at a lower limit set by this noise. If people use voltage or current as electrical signals, they need to use signals larger than the electrical noise of the fluctuating voltage or current. Noise can be observed in various circumstances such as the hissing sound in a telephone, the snowy in a television and unknown pulses in an oscilloscope.

This dissertation follows the style of Sensors and Actuators B.

On the other hand, noise and fluctuations have many applications. Noise can be used as encryptions of signals and image; the drain current flicker noise can be a good monitor for the MOSFET Si-SiO_2 interface quality [1, 2]; resistor noise can be used in various sensor applications.

This dissertation includes two kinds of sensing applications of fluctuation and noise: soil bulk density assessment [3, 4] and bacterium sensing [5, 6].

1.1 Vibration-Induced Conductivity Fluctuation (VICOF) for Soil Bulk Density Extraction

Soil bulk density is the physical property of soils that has many applications in soil studies such as water budgets, nutrient availability, and soil carbon sequestration in plant root zone. These factors involve the growth of plants. However, it is time consuming and difficult to measuring soil bulk density (or porosity) in field conditions. In addition, there are some means to measuring soil bulk density such as volumetric ring, paraffin sealed clod, gamma ray attenuation techniques [7, 8], and Time-Domain Reflectometry (TDR) [9]. However, they are time-consuming, expensive or destructive measurements. To avoid these drawbacks and be available in field conditions, the measurement of Vibration-Induced Conductivity Fluctuation (VICOF) [10] was proposed.

Vibration-Induced Conductivity Fluctuation measures the resistance variation modulated by the vibrations in direct contact with the soil, and provides new information

on soil structure and porosity in addition to electrical conductivity [3, 10]. The advantage of VICOF is the reduced effect of salinity and moisture on the interpretation of Apparent Electrical Conductivity (ECa) applied to other soil properties.

1.1.1 Measurement Setup

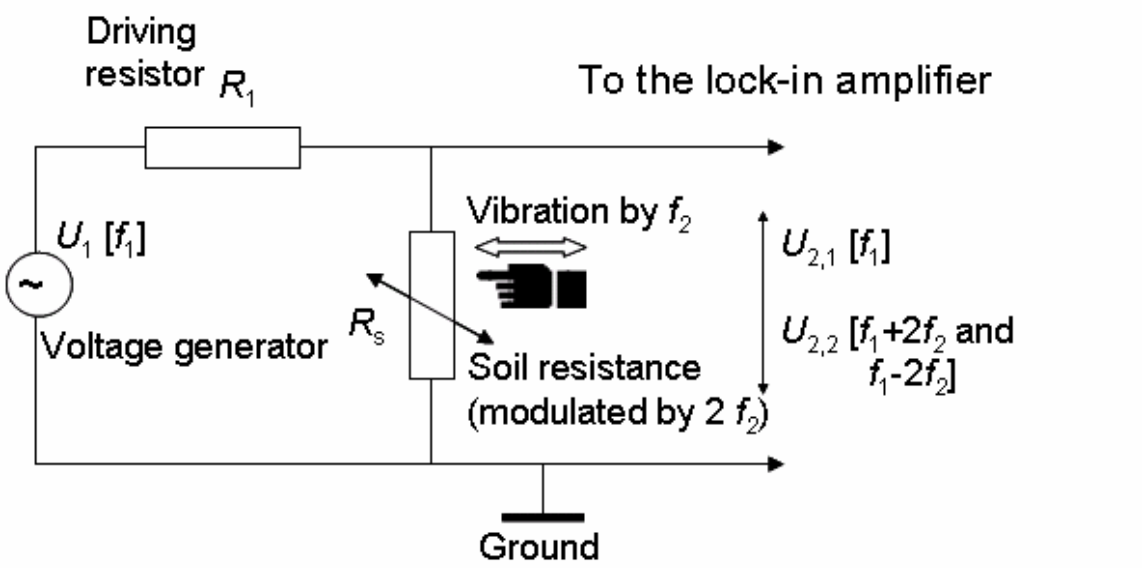

Figure 1.1 Measurement setup

To measure VICOF, the original setup and principles of VICOF were designed. The measurement setup based on the voltage divider circuit is shown in Figure 1.1; "soil sample, sample holder, and electrodes" are shown in Figure 1.2; and vibration method is shown in Figure 1.3. It was the same arrangement as the one used by [10].

This measurement setup was a voltage divider including a AC voltage generator, a driving resistor, a soil resistance, and a lock-in amplifier. The AC voltage generator has AC amplitude of U_1 at frequency f_1 connected with the series resistances (driving resistor R_1 and soil resistance R_s). Due to the applied vibration of the soil samples at frequency f_2, the output voltage across the soil resistance has three major tunes: ac voltage amplitude $U_{2,1}$ at frequency f_1 and AC voltage amplitude $U_{2,2}$, at frequency f_1+2f_2 and f_1-2f_2. Then this output signal is amplified by the lock-in amplifier.

The equations for the AC resistance R_s of the soil sample are shown in the following. The AC resistance of the soil sample (R_s) was calculated from the measurement $U_{2,2}$ in the classical way according to (1).

$$R_s = R_1 \frac{U_{2,1}}{U_1 - U_{2,1}} \tag{1}$$

Supposing the vibration of the soil sample is small, the conductance modulation (dR_s) induced by the periodic vibration and the normalized dR_s/R_s can be estimated from the voltage modulation ($U_{2,2}$) according to the following equations (2) and (3). The detailed deliverance of these equations can be found at [3].

$$dR_s = 2R_1 \frac{U_{2,2}}{U_1 - U_{2,1}} (1 + \frac{U_{2,1}}{U_1 - U_{2,1}}) \ , \tag{2}$$

and

$$\frac{dR_s}{R_s} = 2\frac{U_{2,2}}{U_{2,1}}\left(1+\frac{U_{2,1}}{U_1 - U_{2,1}}\right) \quad . \tag{3}$$

The voltage modulation ($U_{2,2}$) is the difference of the signal $U_{2,2,v}$ signal induced by the vibration and the background voltage ($U_{2,2,0}$) measured without vibration. The magnitude of $U_{2,2,0}$ and $U_{2,2,V}$ is in the order of μV . For the calculation of $U_{2,2}$, the simple difference of $U_{2,2,0}$ and $U_{2,2,V}$ was used in [10, 11], but in the current study, a more precise expression can be obtained from equation (4).

$$U_{2,2} = \sqrt{{U_{2,2,v}}^2 - {U_{2,2,0}}^2} \quad . \tag{4}$$

In the setup of the soil sample, sample holder, and electrodes, the current flow of the electrodes was positioned longitudinally and transversally to the direction of vibration. The sample holder was placed on the floating top of the antivibration table providing that the vibration was horizontal in a well-defined direction.

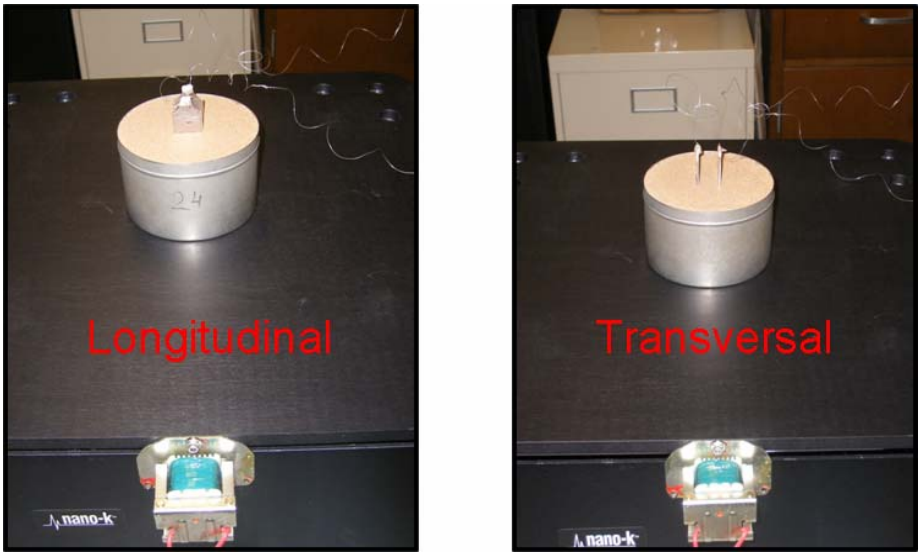

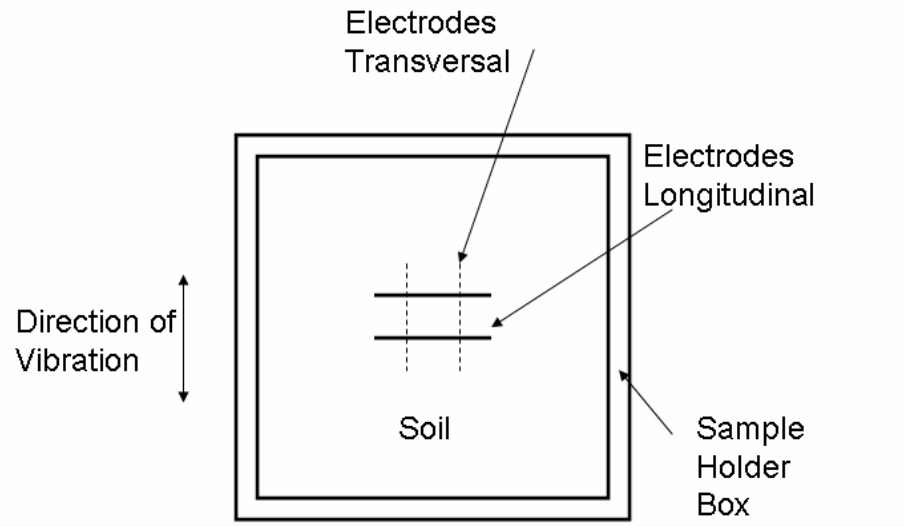

Figure 1.2 Soil sample, sample holder, and electrodes.

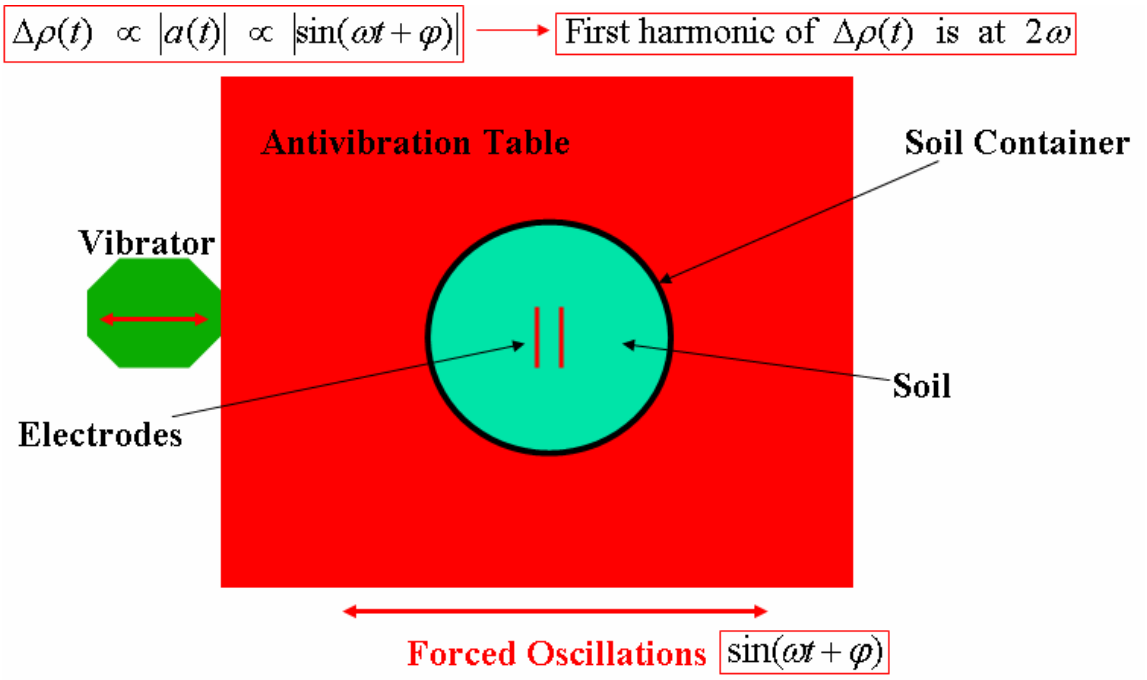

Figure 1.3 Vibration method

In experiments, the soil sample and holder were vibrated by the vibrator at $f_2 = 60Hz$ and generate the first harmonic of $\Delta\rho(t)$ and resistance fluctuation at $2f_2 = 120Hz$. This harmonic will be up-converted by the AC current to $f_1 \pm f_2$ (880Hz and 1.12 kHz). At each longitudinal and transversal position, U_1 and $U_{2,1}$ were measured at 1 kHz and the background $U_{2,2,0}$ and vibration-induced $U_{2,2,V}$ signal were measured at 880Hz and 1.12 kHz. The AC resistance of the soil sample can be obtained from the measurement of $U_{2,2}$. The output measured voltage signal spectrum of VICOF is as shown in Figure 1.4. Both transversal and longitudinal VICOF resistance fluctuations ($dR_{s,T}$ & $dR_{s,L}$) were measured.

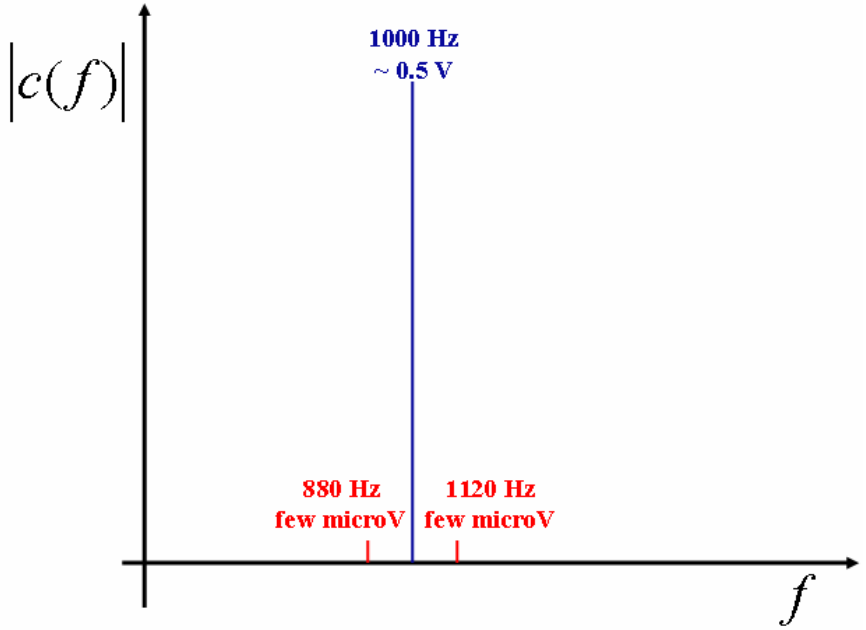

Figure 1.4 Output measured voltage signal spectrum of VICOF

To realize the measurement setup, the block diagram of VICOF measurement was designed, see Figure 1.5. The picture of all VICOF measurement components is shown in Figure 1.6. The details of initial phase of the VICOF study are in A.Sz. Kishné et al, 2007 [3] and the details of the new methods and their theory of VICOF are in Chang et al, 2008 [4].

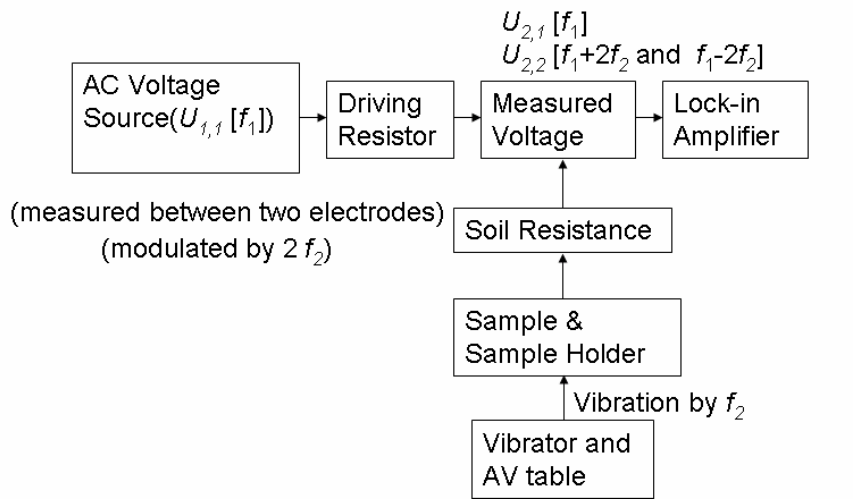

Figure 1.5 Experiment system block diagram of VICOF

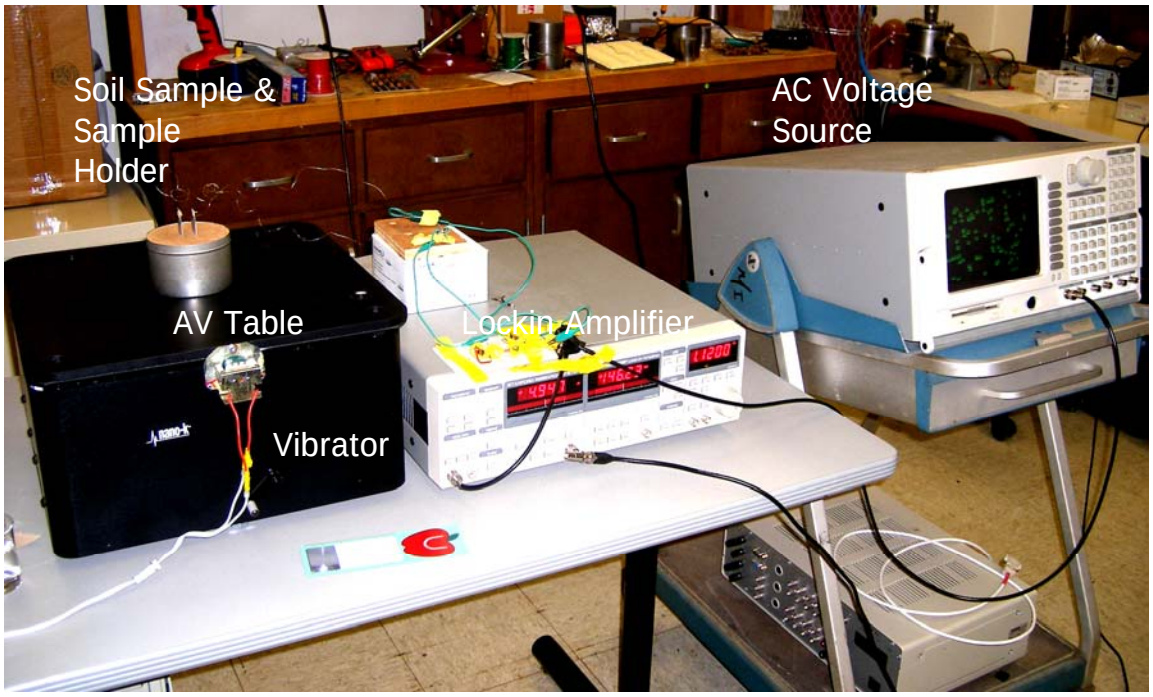

Figure 1.6 Experiment equipment pictures of VICOF

1.2 Fluctuation-Enhanced Sensing (FES) and Binary Pattern for Bacteria

Bacteria detection is an important topic for many areas such as medical science, agriculture, and bio-defense. For medical science and agriculture, bacteria detection can be used to recognize the cause of diseases and identify bacterial contamination. For bio-defense, bacteria detection can keep life from the exposure of biological warfare and prevent damage potential on societies and economies. The rapid evaluation and identification of airborne microorganisms are crucial, especially in case of epidemic preventions and bioterrorist threats.

The ideal bacterial detection method should be fast, sensitive, portable, simple, cheap, practical, and specific. However, the recently available bacterial detection methods often require long culturing periods, expensive and bulky equipment, and trained personnel. One potential way of bacterium sensing is to analyze their odor [12, 13]. Taguchi sensors, meeting the above requirements, could be such candidates of biological sensors.

1.2.1 Fluctuation-Enhanced Sensing (FES) for Bacteria

1.2.1.1 Fluctuation-Enhanced Sensing (FES)

To enhance the sensitivity and selectivity of gas sensors, Fluctuation-Enhanced Sensing (FES) [5, 14, 15-29] was used. Fluctuation-Enhanced Sensing is a method to

amplify, measure, and analyze the small stochastic component of the sensor signal (stochastic fluctuations) influenced by chemical environment. The gas molecule fragments move randomly along the grain boundary; therefore, their conductance modulation effect is time dependent with a stochastic nature. Because the doping properties and the diffusion constant of the fragments are specific for each chemical agent, the induced conductance noise has the fingerprint of the chemical agent.

The most conventional way of using FES is to measure the power density spectrum (noise spectrum) of the stochastic signal components. In this study, this conventional way of FES was used to improve the sensitivity, selectivity, and reproducibility of Taguchi sensors.

Taguchi sensors, which are commercially available, are heated semiconductor oxide films (usually SnO_2) with broad applications, including safety monitors for detecting combustible, pollution, and toxic gases. The operation principle of Taguchi sensors is based on the change of the sensor resistance because the gaseous agent diffuses into the film, breaks into molecular fragments, and at the grain boundaries, it changes the conductivity of intergrain junctions by acting as an electron donor or acceptor. Multiple gas identification can be done with single sensors [5, 30-34] with temperature modulation but with limited selectivity [35, 36]. To get a better selectivity to identify gas mixtures, arrays of different sensors are used. The typical devices are sensor systems combined with a pattern recognition unit, so-called "Electronic Nose [37-40]" (EN, for odors) or "Electronic Tongue" (ET, for liquid phase). Recently, ENs and ETs have been applied in various fields including environmental, agricultural, and medical

applications, and also in the food, beverage, and automotive industries. The test personnel can use these devices instead of their own noses and tongues. They can also be used as quantitative tools to detect and identify of bacteria and to prevent the test personnel from exposure to the agents.

For Taguchi sensors, two ways of FES are used:

i. Regular sensing (RS) method. In this case, the sensors are heated constantly during the measurement. To avoid excess noises from temperature fluctuations caused by the air flow turbulence, there is no air flow during the data collection.

ii. Sampling-and-hold (SH) method. In this case, the sensor is heated for several minutes. During the heating process, air flow is optional. Then the heater (and gas flow) is/are turned off. After the sensor cooled down, the stochastic signal is recorded. In this case, the gas fragments are trapped in the film and escape slowly. Consequently, the measurement can also be taken later. Another advantage of this method is that the noise induced by temperature fluctuations due to microscopic turbulence in the hot air convection can be avoided.

1.2.1.2 Sensors and Samples

In this dissertation, the power density spectra of three commercial Taguchi gas sensors: Sensors SP32, SP11, TGS2611 (see Figure 1.12) were used to identify four biological samples composed of the combination of two types of bacteria: Escherichia Coli (E. coli) and Anthrax-surrogate *Bacillus subtilis* (Anthrax) (see Figure 1.13) and

their culture medium Tryptic Soy Agar (TSA). In the following content of the dissertation, the alias "E. coli", "Anthrax", and “TSA” stand for Escherichia Coli, Anthrax Surrogate *Bacillus Subtilis*, and Tryptic Soy Agar respectively. These four biological samples were TSA, TSA+ E.coli, TSA+ Anthrax, and TSA+ E.coli + Anthrax. The details of the sample preparation are shown in Chang et al, 2009 [5].

1.2.2. Measurement Setup of Fluctuation-Enhanced Sensing

Two devices were used in this study: non-portable and portable devices. Section 1.2.2.1 shows the measurement setup of the non-portable device and Section 1.2.2.2 shows the measurement setup of the portable device. On one hand, the non-portable device was heavy and expensive, and it can only be used in the laboratory. On the other hand, the portable device was light and cheap, and it can be used anywhere with a laptop.

1.2.2.1 Non-Portable Device

This section demonstrates the fluctuation-enhanced odor sensing system, which is the non-portable device used only in a laboratory for its heavy and expensive equipments. The concept of this device is that the sensors and samples are put in the same chamber and the sensor can detect the odor of the samples that accumulate in the chamber.

The measurement circuitry is a voltage divider (see Figure 1.7), where U_0 is the driving DC voltage, U_s is the measured DC voltage of sensor, $R_L = 36\,\mathrm{k}\Omega$ is the serial resistor and R_s is the actual resistance of the measured sensor. The normalized power density spectrum $S_r(f)/R_s^2$ can be derived from the equations below.

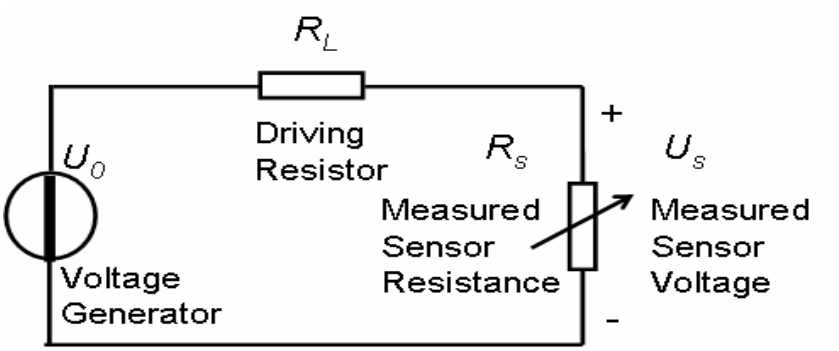

Figure 1.7 Measurement circuitry

The relationship between the applied DC voltage U_0 and measured sensor voltage U_s can be obtained from the relationship of the voltage divider:

$$U_s = U_0 \frac{R_s}{R_L + R_s} \quad . \tag{5}$$

Then the evaluation formula for the actual resistance of the measured sensor is

$$R_s = R_L \frac{U_s}{U_0 - U_s} \quad . \tag{6}$$

Furthermore, a parameter ε is defined:

$$\varepsilon = \frac{dU_s}{dR_s} = U_0 \frac{R_L}{(R_L + R_s)^2} \quad . \tag{7}$$

Therefore, the relationship between $S_r(f)$, the mean-square resistance fluctuations dR_s^2 of the sensor in an infinitesimally small df bandwidth, the measured mean-square voltage fluctuations in df bandwidth, and the measured $S_u(f)$ (raw power spectra) are as follow:

$$S_r(f)df = dR_s^2 = \frac{dU_s^2}{\varepsilon^2} = \frac{S_u(f)}{\varepsilon^2}df \quad . \tag{8}$$

Consequently:

$$S_r(f) = \frac{S_u(f)}{\varepsilon^2} = \frac{S_u(f)}{U_0^2}\left[\frac{(R_L + R_s)^2}{R_L}\right]^2 \tag{9}$$

In conclusion, the normalized power density spectrum can be determined from the measured voltage spectrum $S_u(f)$ with the following equation:

$$\frac{S_r(f)}{R_s^2} = \frac{S_u(f)}{U_0^2}\left[\frac{(R_L + R_s)^2}{R_L R_s}\right]^2 \tag{10}$$

This normalization do not influence the pattern generation in Section 3.4 and in Chang et al, 2008 [6].

To realize the measurement setup, the measurement system block diagram was established, see Figure 1.2.2. The system included the following components: a power supply, a low noise current generator, a preamplifier, a power spectrum analyzer, a grounded stainless steel sensor chamber, Taguchi sensors, and test samples. The pictures of all components are shown in Figures 1.9~13. The following are the setup of this device.

The sensors were placed in the grounded stainless steel sensor chamber (volume 700 cm^3) where the odors generated by the samples could accumulate. These sensors were heated by the stable power supply (XP650) and the low noise current generator drove the sensors' resistors with low-noise DC current. The induced voltage fluctuations were amplified by the preamplifier (SR560 Low Noise Preamplifier). The power spectra of the amplified voltage noise across the sensors were measured by the power spectrum analyzer (SR785 Dynamic Signal Analyzer) or by the DSP system (DSP Data Acquisition System (DAS 1614SD)) and the software written by Labview. The power spectrum of the voltage fluctuation was measured in the frequency range 100Hz~100kHz.

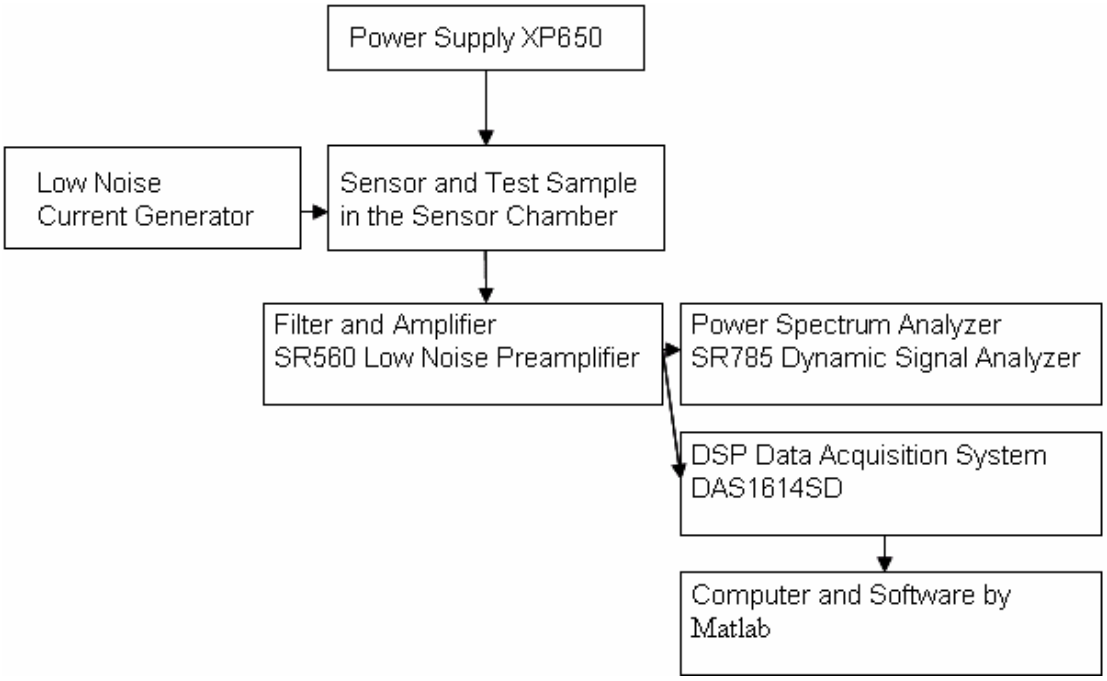

Figure 1.8 Fluctuation-enhanced odor sensing system

Figure 1.9 Filter and amplifier

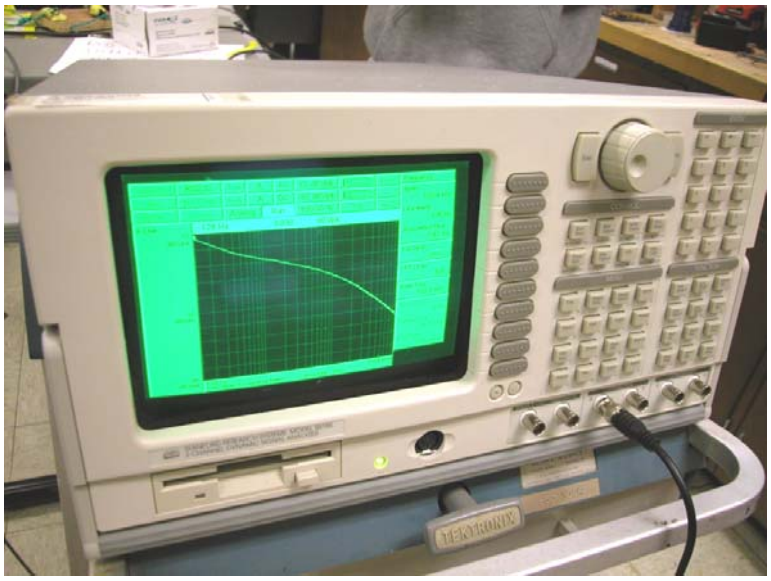

Figure 1.10 Power spectrum analyzer

Figure 1.11 Grounded stainless steel sensor chamber

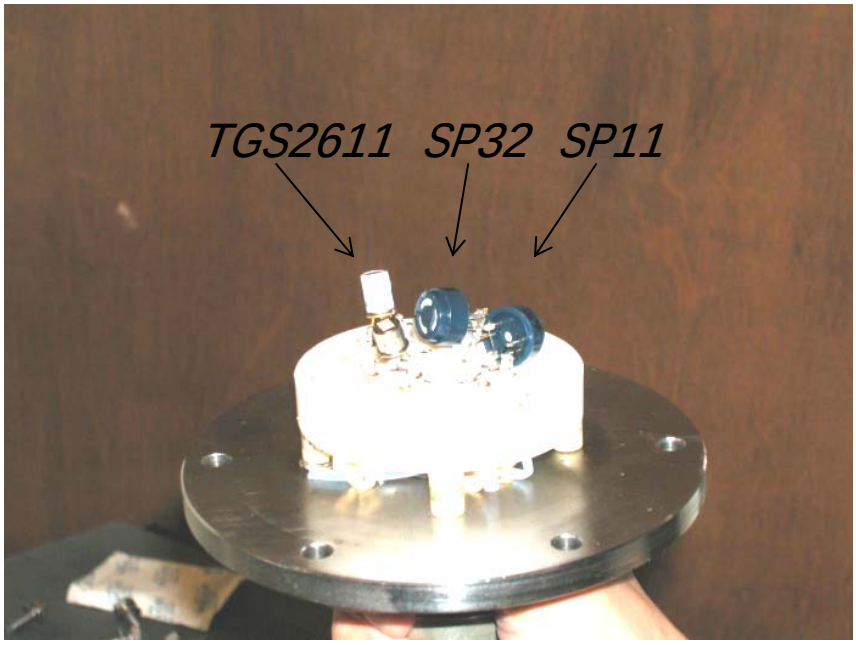

Figure 1.12 Taguchi sensors

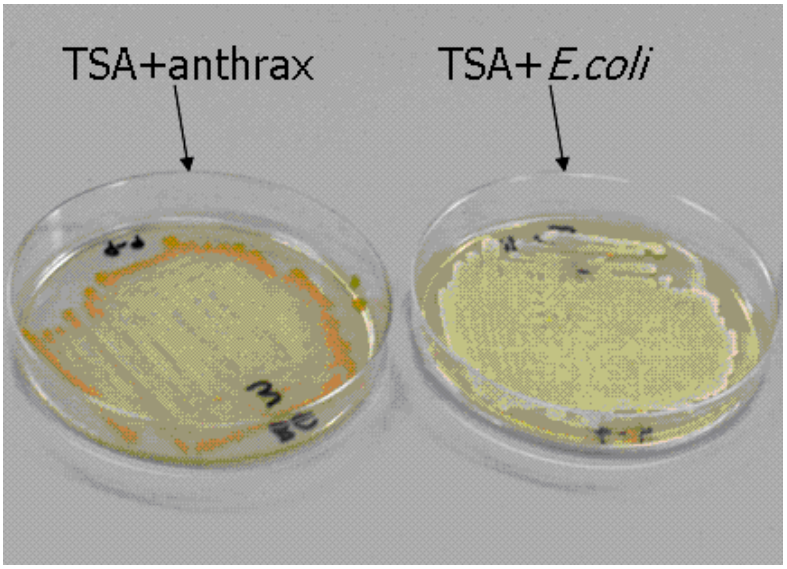

Figure 1.13 Test samples

1.2.2.2 Portable Device

The former section described the non-portable device that can be used in a laboratory only. In the research project (army research project), a portable device was designed and built (in an international collaboration mainly by the University of Szeged, Hungary) to be used anywhere with a laptop. The concept of the portable device is that the device can inhale gas and odors, detect odors by its sensors and then transfer the data to a computer.

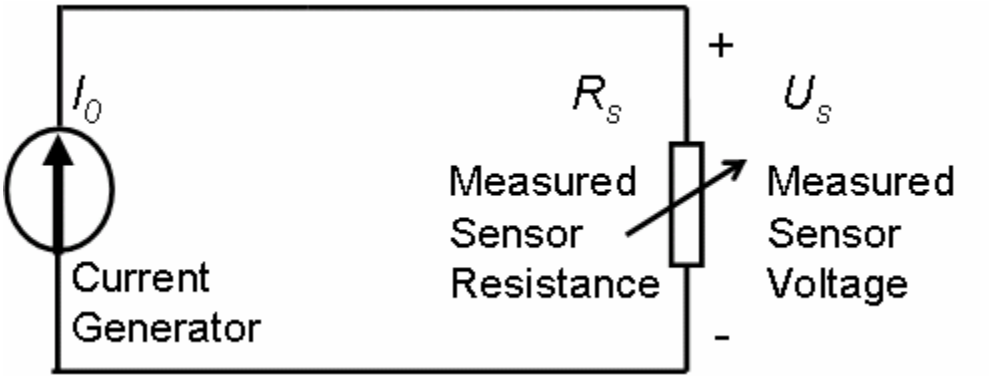

Figure 1.14 Circuitry of portable device

The circuitry of the portable device shown in Figure 1.14 is a current source I_0 (controlled by the GSA software for windows) connected with a Taguchi sensor. The measured sensor voltage and resistance of the Taguchi sensor is U_s and R_s . This current source is assumed to be ideal and constant; therefore, the measured sensor resistance can be obtained directly from the following equation.

$$R_s = \frac{U_s}{I_0} \tag{11}$$

Similarly, the relationship between the measured voltage spectrum $S_u(f)$ and measured resistance spectrum $S_r(f)$ can be obtained from (12).

$$S_r(f) = \frac{S_u(f)}{I_0^2} \tag{12}$$

The picture of the portable device and additional components are shown in Figure 1.15 and the block diagram of the portable device is shown in Figure 1.16. This device includes the following components: pumps, a diffuser, an air inlet, sensors, a preamplifier, and sensor drivers. The following are the functions of these components.

The pumps were used to generate the air flow to inhale the odor generated by the sample. The diffuser and the air inlet constructed a tunnel for the gas to enter the chamber of the portable device. The sensors were the same Taguchi sensors used in the non-portable device. The sensor drivers were used to control the heater voltage and current generator. The preamp was used to amplify the fluctuation signals generated by the sensors. A computer could control the portable device via the "GSA" software including the following functions: the pumps' on/off switches, the bias current of the sensors, and the amplification of the preamp. This software could also transfer the

fluctuation signals to a computer and convert the time data into power spectra ($S_u(f)$ or $S_r(f)$).

However, this device had poor sensitivity and needed additional components to enhance its sensitivity. The odor of sample could not accumulate, because this device had no chamber. Therefore, a bag was needed to contain the sample inside and accumulate the odors generated by the samples, which worked the same as the grounded stainless steel sensor chamber in the non-portable device. After several minutes, the bag accumulated enough odor generated by the sample, the device could inhale the gas of the bag to its chamber. Also, the device could leak the inhaled gas from the pump side and reduce the odor concentration of the chamber. To prevent this leakage, a shutter was needed in the pump side. After the device inhaled the gas in the bag, the shutter had to seal the pump side immediately.

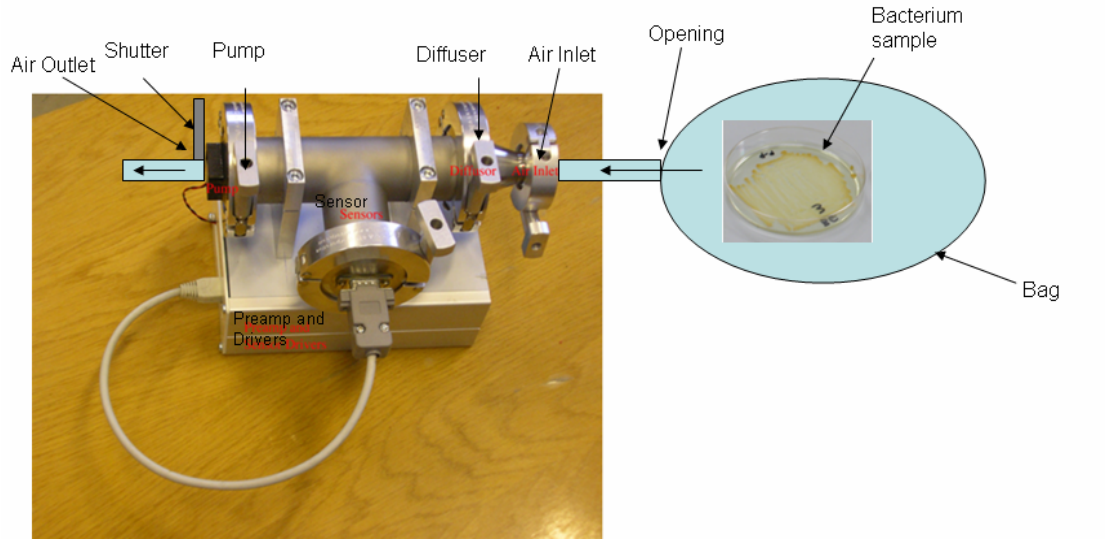

Figure 1.15 Portable device and additional components

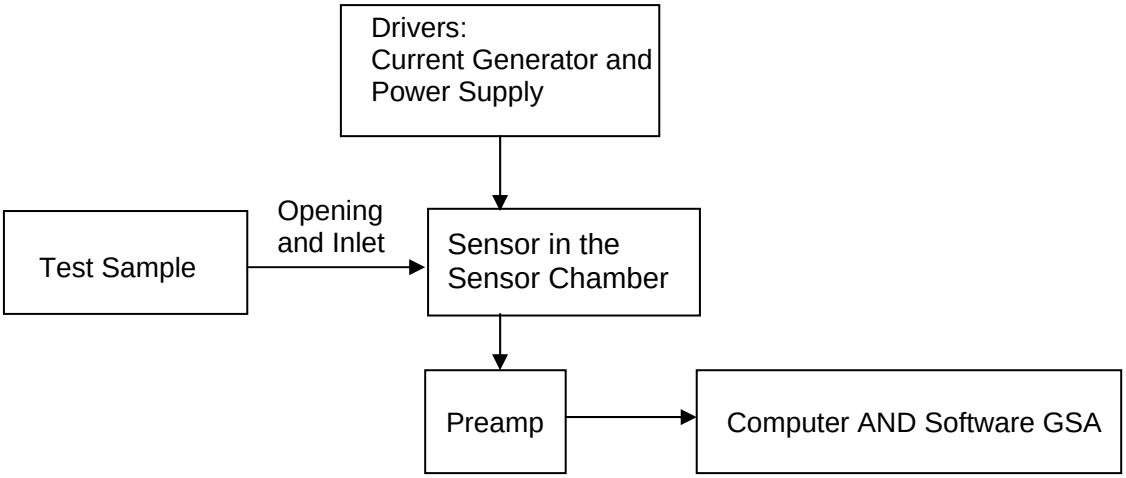

Figure 1.16 Block diagram of portable device

Even with these modifications, the portable device still has deficiencies. The distance between the sensors is distant (~40cm) from the samples that reduce the sensitivity and selectivity of the device. Further, the portable device cannot measure in sampling-and-hold mode. In sampling-and-hold mode, the sensor resistance is large (~500kohm). Even though the minimum current source ($8.3\mu A$) is used in this portable device, the measured voltages of the sensors are still overloaded. In contrast, the non-portable device uses a voltage source; therefore, the measured voltage cannot be overloaded. The results of the portable device are shown in Section 3.3.2.

1.2.3 Binary Pattern for Bacteria

To design a system for bacterium recognition with ultra-low power consumption, the usage of microprocessors and extensive data processing must be avoided. The sensor signals must be processed in the simplest possible way, presumably with analog circuitries, and the pattern recognition must be a deterministic process based on a few simple logic decisions. Consequently, the new method to generate binary patterns was proposed. In order to demonstrate the feasibility of the method and the nature of binary patterns, relevant experimental tests and evaluations were conducted and results are shown in Sections 3.3~4.

2. SUMMARY OF VIBRATION-INDUCED CONDUCTIVITY FLUCTUATION (VICOF) RESULTS*

This section summarizes the results of Vibration-Induced Conductivity Fluctuation (VICOF) study, including two sections: Original Developments in Kishné et al, 2007 [3] and New Methods and Their Theory in Chang et al, 2008 [4].

2.1 Original Developments

Kishné et al, 2007 [3] demonstrates the original developments of VICOF including the methodology, simulation, samples and their treatments, and experiment results of VICOF. In summary, the blade electrodes have better performance than the cylindrical electrode, because the blade electrodes have less set-up noise in the measurement of normalized vibration-induce conductivity (VICOF).

In addition, the theory, computer simulations, and measurement results in this dissertation elucidate that the ratio of transversal/longitudinal normalized VICOF is independent of moisture and salinity affects. In other words, soil moisture and soil salinity do not affect the normalized VICOF signal. However, these experimental data have large scattering [3] due to the loose and heavy contacts. Therefore, the new methods and schemes are proposed in Chang et al, 2008 to solve the effect of the poor contacts.

2.2 New Methods and Their Theory

Chang et al, 2008 [4] presents new VICOF methods, arrangements, and schemes of VICOF. The new VICOF methods of electromechanical response illustrate the relationship between applied vibrations, stress and strain, resistance, and resistance variation. Based on the methods, arrangements, and schemes of VICOF for both laboratory and field measurements were invented.

The following is the comparison between the original and the new developments. The original arrangement [3] is a two-point measurement; and the new arrangement is a four-electrode measurement with line or plate contacts. The original VICOF schemes [3] have only horizontal vibration in the transversal and the longitudinal directions of the current flow; and the new schemes have additional vertical vibration and compression VICOF in the transversal directions of the current flow.

The new schemes and arrangements provide two advantages; the applied force can be perpendicular to the current, and the exact value of the soil resistivity can be derived directly. Besides the former advantage, the vertical vibration and compression can minimize the loose electrode impacts on the measurement in accuracy and reproducibility.

3. RESULTS OF FLUCTUATION-ENHANCED SENSING*

This section demonstrates both the published and unpublished results of the bacterial sensing study, including the non-portable and the portable device measurement procedures, measurement results, and the method to generate continuous pattern and binary pattern extracted from experiment results. To enhance the sensitivity, selectivity, and reproducibility of sensors, two devices (non-portable and portable device) and two methods of analysis (power spectra obtained by the power spectrum analyzer and power spectra converted from the time data by the software written by Matlab) were used.

After that, the study to generate the continuous pattern and the binary pattern was designed to find a way to generate patterns with perfect reproducibility based on the spectral slopes in different frequency ranges at FES. The obtained binary patterns can be used at a microprocessor-free system using building elements of analog circuitries and a few logic gates with ultra low power consumption in Chang et al, 2010 [6].

3.1 Measurement Procedures

This section illustrates the measurement procedures for two devices: non-portable and portable device.

3.1.1 Non-Portable Device

For all test samples, the power spectra of all the sensors over the measured frequency range were roughly as 1/f. The sensor resistance was ohmic in the observed range of DC voltage (0.3-6V). The measured power density spectrum of the output voltage is proportional to the square of the DC voltage which confirms the resistance fluctuations origin of the voltage fluctuations [41, 42].

To enhance the selectivity and sensitivity of sensors, all sensors were measured both by the constantly heated (heated) FES [14, 31] and the sampling-and-hold [32, 33] FES methods. In the heated case, the nominal heating voltage (5V) was applied during the whole measurement. After the sample was placed in the chamber and the chamber was closed, the chamber was flushed with synthetic air for 3 minutes. After a stable odor was obtained (typically 5 minutes), the corresponding stable spectrum was developed. The measurements often take 3 minutes.

Each sampling-and-hold measurement [32, 33] was preceded by a heated FES measurement sequence with stationary heating. Then, to execute the sampling-and-hold FES measurement, the heating was turned off while the spectrum was monitored. After 5

minutes, if the spectrum was stable, the spectrum was recorded, which was the output pattern of the sampling-and-hold measurement [32, 33]. The measurements also took 3 minutes.

Because the sensitivity of the system against resistance fluctuation depends on the value of the series resistance providing the battery-driven DC current drive for the sensor bias, whenever the measured voltage fluctuation were too small and close to the baseline, these resistors were changed for a proper one yielding sufficiently large FES signals.

Five conditions were tested in non-portable device experiments: empty chamber, TSA only, TSA + E. coli, TSA + Anthrax, and TSA + E. coli + Anthrax. After removing the sample, the sensor was heated clean for 10 minutes and the chamber was flushed with synthetic air for 3 minutes. To see the reproducibility of the spectra, after completing the whole sequence of the experiments with all the different samples, the whole sequence of tests with all the samples was repeated. In a few cases, the samples were re-tested two or four times. The following is the example of the non-portable device experiment schedule.

Table 3.1 Example of the schedule of non-portable device experiment

Time	Chamber Condition	Sample in Chamber	measurement data
3min	heated sensor	Empty	heated measurement
5min	Sampling-and-hold sensor	Empty	
3min	Sampling-and-hold sensor	Empty	Sampling-and-hold measurement
5min	heated sensor	TSA	
3min	heated sensor	TSA	heated measurement
5min	Sampling-and-hold sensor	TSA	
3min	Sampling-and-hold sensor	TSA	Sampling-and-hold measurement
7min	heating clean	Empty	
3min	Heating clean and Synthetic Air Flushing	Empty	
5min	heated sensor	TSA+ E.coli	
3min	heated sensor	TSA+ E.coli	heated measurement
5min	Sampling-and-hold sensor	TSA+ E.coli	
3min	Sampling-and-hold sensor	TSA+ E.coli	Sampling-and-hold measurement
7min	heating clean	Empty	
3min	Heating clean and Synthetic Air Flushing	Empty	
5min	heated sensor	TSA	
3min	heated sensor	TSA	heated measurement
5min	Sampling-and-hold sensor	TSA	
3min	Sampling-and-hold sensor	TSA	Sampling-and-hold measurement
7min	heating clean	empty	
3min	Heating clean and Synthetic Air Flushing	empty	
5min	heated sensor	TSA	
3min	heated sensor	TSA	heated measurement
5min	Sampling-and-hold sensor	TSA	
3min	Sampling-and-hold sensor	TSA	Sampling-and-hold measurement
7min	heating clean	empty	
3min	Heating clean and Synthetic Air Flushing	empty	
5min	heated sensor	TSA+ Anthrax	
3min	heated sensor	TSA+ Anthrax	heated measurement
5min	Sampling-and-hold sensor	TSA+ Anthrax	
3min	Sampling-and-hold sensor	TSA+ Anthrax	Sampling-and-hold measurement
7min	heating clean	empty	
3min	Heating clean and Synthetic Air Flushing	empty	
3min	heated	empty	heated measurement
5min	Sampling-and-hold	empty	
3min	Sampling-and-hold	empty	Sampling-and-hold measurement
7min	heating clean	empty	
3min	Heating clean and Synthetic Air Flushing	empty	

3.1.2 Portable Device

The observed frequency range of measured power spectra and observed resistance range were 1/f (100~100KHz for the power spectrum analyzer) and ohmic, which is the same as these of the non-portable device. Unlike the non-portable device, the sensors in this portable device can only measure in constantly heated (heated) FES mode.

The nominal heating voltage (3V) was applied during the whole measurement. After the sample was placed in the plastic bag for 3 minutes and the bag accumulated enough sample odor, the device pumped the gas inside the bag, turned off the pump, the shutter sealed pump side. Until a stable odor inside the device (typically 1 minute), the corresponding stable spectrum was developed. After that, the spectrum was recorded.

Because the sensitivity of the system against resistance fluctuation depends on the driven DC current drive for the sensor bias, whenever the measured voltage fluctuation were too small and close to the baseline, the driving current was changed for a proper one yielding sufficient large FES signals.

As with non-portable device, five conditions were tested in these experiments: empty chamber, TSA only, TSA + E. coli, TSA + Anthrax, and TSA + E. coli + Anthrax. After removing the bag and sample, the shutter opened. To clean the device, the sensors were heated, and the chamber of the portable device was flushed with air for 3 minutes. To see the reproducibility of the spectra, the whole sequence of the experiments was repeated. The following is the example of the portable device experiment procedure.

Table 3.2 Example of the schedule of portable device experiment

Time	Chamber Condition	Inlet	measurement data
3min	heated sensor	empty bag	heated measurement
3min	heated sensor	TSA	
1min	heated sensor	TSA	heated measurement
3min	Heating clean and Synthetic Air Flushing	empty	
3min	heated sensor	TSA+ E.coli	
1min	heated sensor	TSA+ E.coli	heated measurement
3min	Heating clean and Synthetic Air Flushing	empty	
3min	heated sensor	TSA	
1min	heated sensor	TSA	heated measurement
3min	Heating clean and Synthetic Air Flushing	empty bag	
3min	heated sensor	TSA+ Anthrax	
1min	heated sensor	TSA+ Anthrax	heated measurement
3min	Heating clean and Synthetic Air Flushing	empty	
3min	heated sensor	empty	heated measurement

3.2 Measurement Results

This section presents the measurement results of the raw power spectra of Fluctuation-Enhanced Sensing with the non-portable device and the portable device. The raw power spectra of the non-portable device are $S_u(V^2/Hz)$ and the raw power spectra of the non-portable device are $S_r(\Omega^2/Hz)$.

3.2.1 Non-Portable Device

Two methods were used to obtain the experiment results: spectral data from the power spectrum analyzer and spectral data converted from time data by the software written by Matlab. The time data are the raw data of voltage fluctuation of the sensor

resistance, which can be obtained by DSP Data Acquisition System. The spectral data are the Fourier transform of the time data, which can be directly obtained by the power spectrum analyzer or obtained by the software written by Matlab. This software can convert the time data (from DSP Data Acquisition System) into spectral data.

3.2.1.1 Results from Spectra Analyzer

The following are the results of the spectral data from the power spectrum analyzer. The raw power spectra of SP32, TGS 2611, and SP11 for both the heated and sampling-and-hold sensor measurements are shown in Figures 3.1 to 3.6 Good reproducibility and negligible memory effects are indicated by the fact that the spectra obtained with the same sensor in the empty chamber, before and after measurements with the samples in the chamber, practically overlap each other. Similarly, the spectra of the same sample measured by the same sensor also show good reproducibility.

In Figure 3.1, the raw spectra measured with the sensor SP32 in the heated mode are shown. The power spectra can be clearly divided into three groups: Empty; TSA; TSA + Anthrax, and TSA + *E. coli*, which means TSA + Anthrax and TSA + E. coli are indistinguishable. Although in this figure the spectra of these two bacteria sample can split a little bit, they often overlap each other in other experiments.

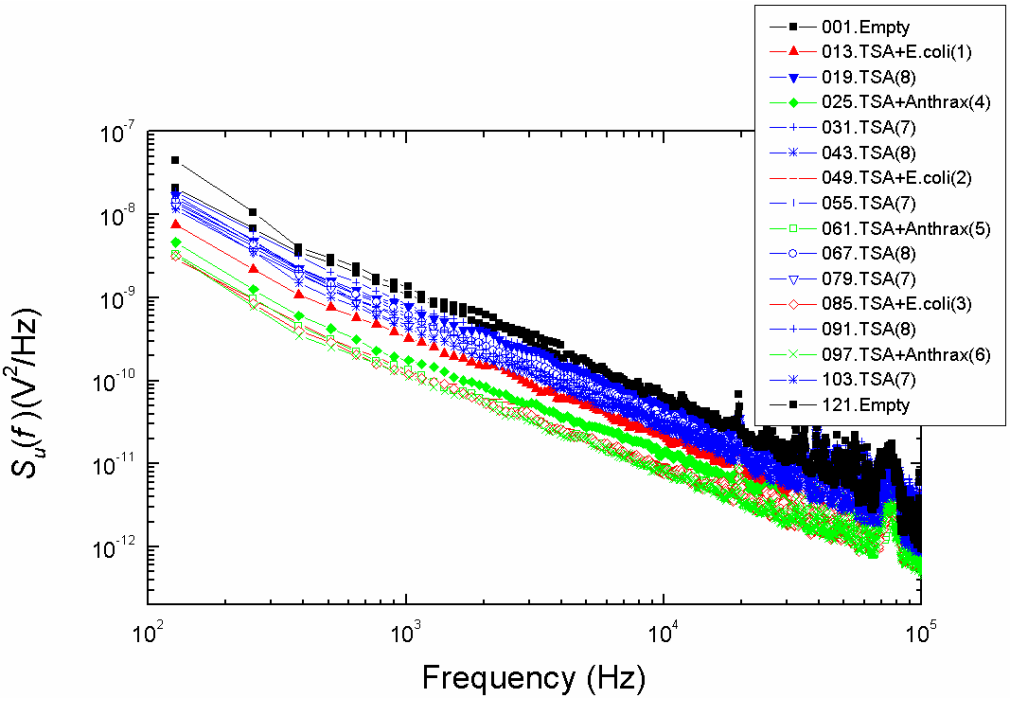

Figure 3.1 Raw power spectra of the heated sensor SP32 (non-portable device) obtained by the power spectrum analyzer

In the sampling-and-hold working mode, most of the spectra obtained with the sensor SP32 are also well distinguishable, see Figure 3.2, except the measurements with the two bacteria (*E. coli* and Anthrax) yielding similar patterns.

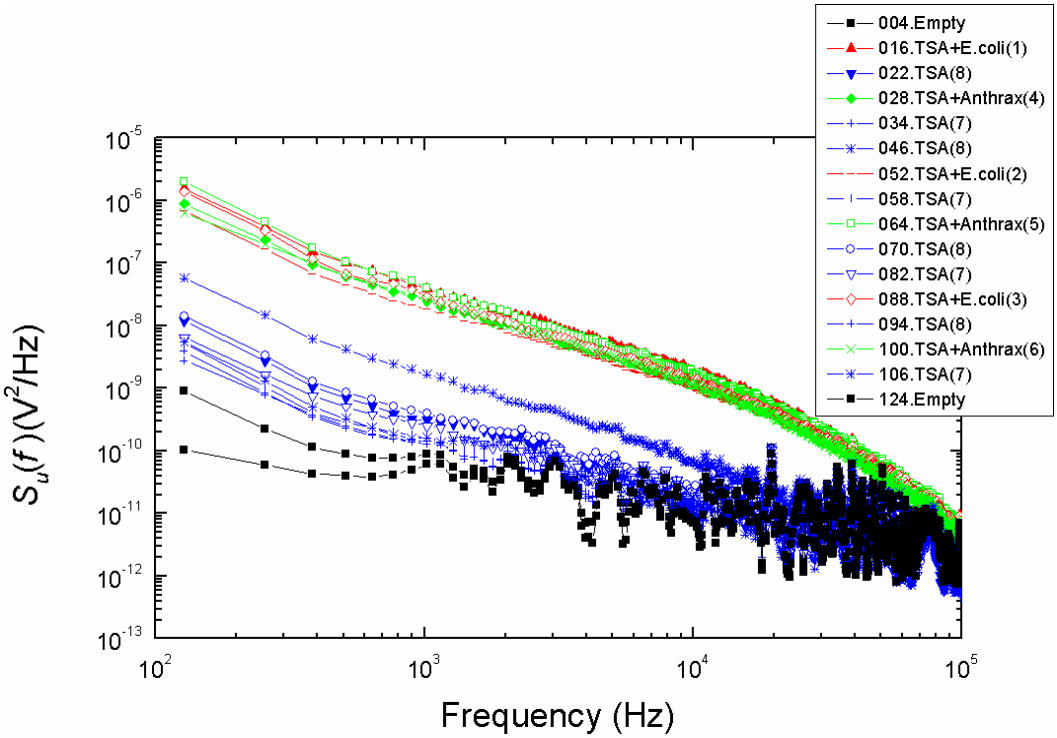

Figure 3.2 Raw power spectra of the sampling-and-hold sensor SP32 (non-portable device) obtained by the power spectrum analyzer

In Figure 3.3, the raw spectra measured with the sensor TGS 2611 in the heated mode are shown. The spectra cannot be clearly differentiated due to large variations and overlaps.

In the sampling-and-hold mode (see Figure 3.4), the plot of the raw spectra of the sensor TGS2611 can clearly be divided into two groups: Empty and TSA; and TSA + Anthrax and TSA + *E. coli*, respectively. That means, the empty chamber and the chamber with the TSA, bacterium types are indistinguishable. Compared with the result

of the heated sensor, the sampling-and-hold method can enhance the selectivity and sensitivity of this sensor.

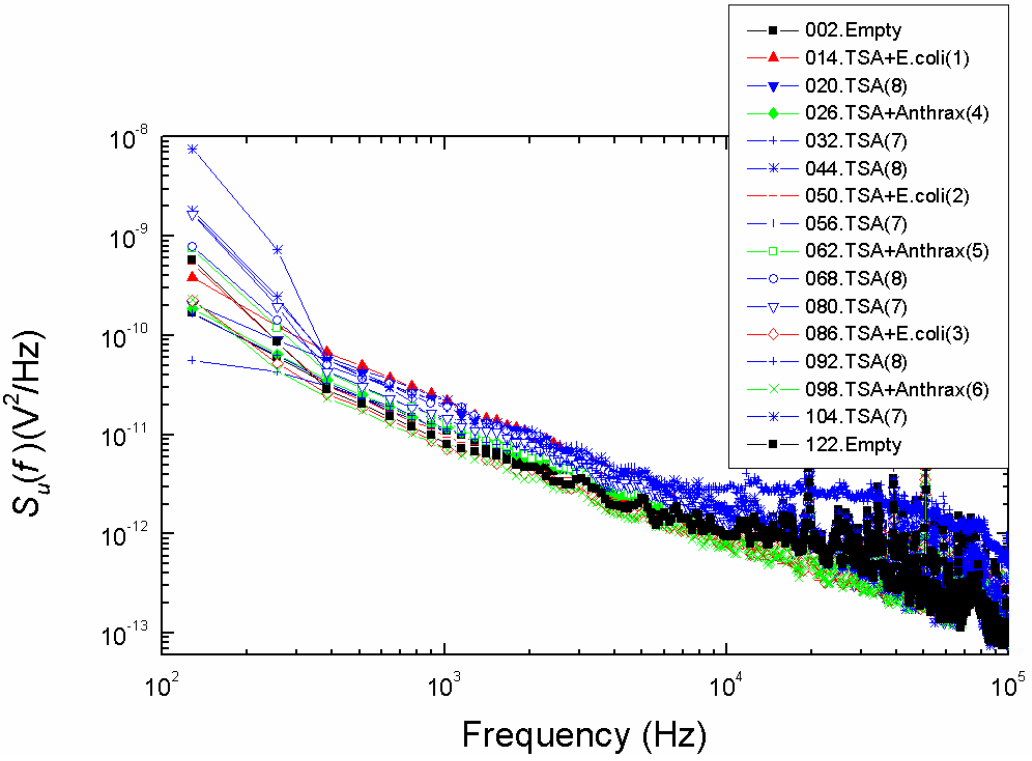

Figure 3.3 Raw power spectra of the heated sensor TGS 2611 (non-portable device) obtained by the power spectrum analyzer

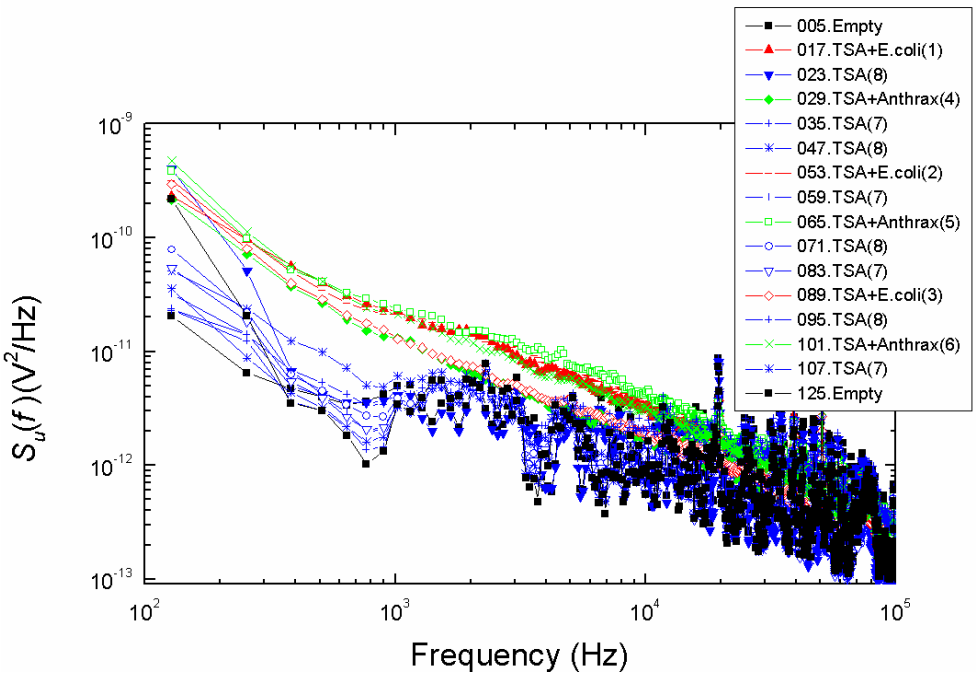

Figure 3.4 Raw power spectra of the sampling-and-hold sensor TGS 2611 (non-portable device) obtained by the power spectrum analyzer

In Figure 3.5, the raw spectra measured with the sensor SP11 in the heated mode are shown. The spectra can be clearly divided into two groups: Empty and TSA; and TSA + Anthrax and TSA + *E. coli*. The empty chamber and the chamber with the TSA are indistinguishable just like the two bacteria from each other. This is fine for the detection of the presence of bacteria but not for their separate identification.

In Figure 3.6, the spectra measured with the sensor SP11 in the sampling-and-hold mode are shown. The *shapes* of the raw spectral patterns, even though they overlap in several ranges, can clearly be divided into three groups: Empty; TSA; and TSA + Anthrax and TSA + *E. coli*.

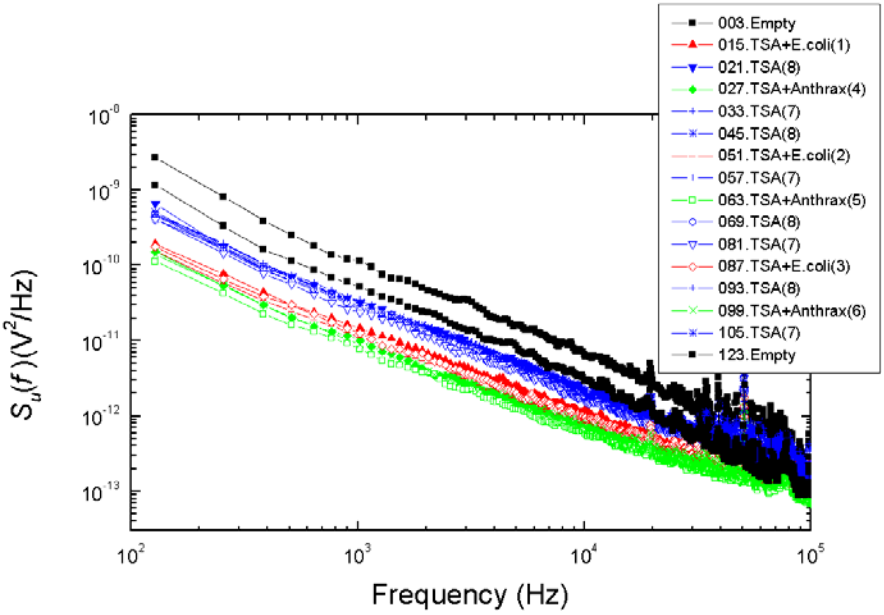

Figure 3.5 Raw power spectra of the heated sensor SP11 (non-portable device) obtained by the power spectrum analyzer

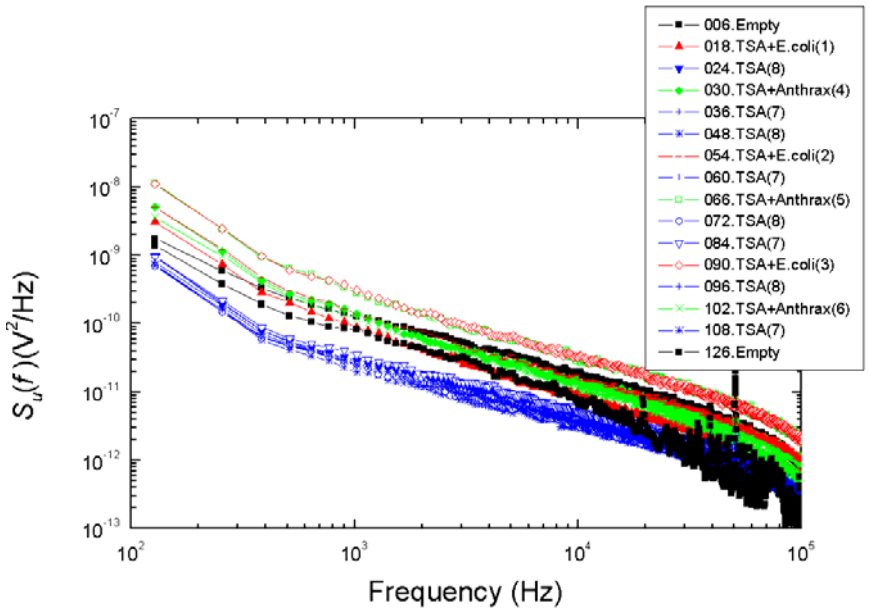

Figure 3.6 Raw power spectra of the sampling-and-hold sensor SP11 (non-portable device) obtained by the power spectrum analyzer

The conclusions of this exploratory study about the feasibility and reproducibility of using Fluctuation-Enhanced Sensing with single Taguchi gas sensors to detect and identify different bacteria are summarized in Table 3.3. Sensors in sampling-and-hold mode have better detectability than in heated mode. In addition, advanced stochastic signal analysis at the time data level [28] is a powerful tool and has potentials to further enhance the detectability of this type of sensing, which is discussed in Section 3.2.1.1.

Table 3.3 Summary of raw power spectra (non-portable device) obtained by the power spectrum analyzer: + well detected/identified/repeatable; x unrecognizable/non-repeatable

Sensor	FES Mode	w/o Bacteria	empty/TSA	Bacteria Type
SP 32	Heated	+	+	x
SP 32	Sampling-and-hold	+	+	x
TGS 2611	Heated	x	x	x
TGS 2611	Sampling-and-hold	+	x	x
SP 11	Heated	+	x	x
SP 11	Sampling-and-hold	+	+	x

3.2.1.2 Results from DSP Data Acquisition System and the Software Written by Matlab

This method is used to analyze the results of sensors in sampling-and-hold mode only because sensors operated in this mode can yield good selectivity. The results of spectral data converted from the time data by the software written by Matlab are shown in Figures 3.7 to 3.9. The amplitudes of the power spectra are amplified by gain square ($500^2 = 250000$).

The spectra of all the sensors: SP32, TGS 2611, and SP11 can be divided into three groups Empty; TSA; and TSA + Anthrax, TSA + *E. coli*, and TSA + Anthrax + *E. coli*. The results are summarized in Table 3.4. The results of sensors SP32 and SP11 obtained by this method are as well as these obtained by the power spectrum analyzer. However, the results of the sensor TGS 2611 obtained with this method are better than those obtained with the power spectrum analyzer (only two groups Empty and TSA; TSA + Anthrax and TSA + *E. coli*).

This method can enhance the sensitivity and selectivity more than the former method (spectra obtained by the power spectrum analyzer). However, this method is very time consuming because obtaining time-data measurements takes a lot of time. It took 1 minute to measure a spectrum with the former method; and it took 5 minutes to measure a spectrum with latter method. Therefore, the power spectrum analyzer was used in most of the experiments in this dissertation.

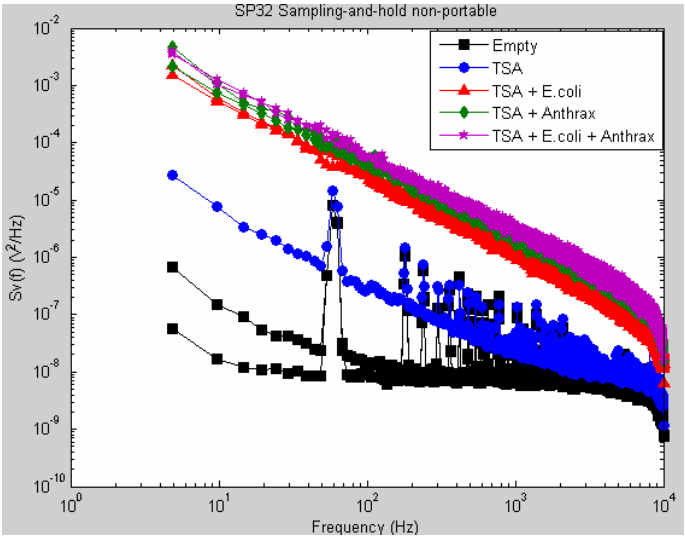

Figure 3.7 Raw power spectra of the sampling-and-hold sensor SP32 (non-portable device) converted by the software written by Matlab

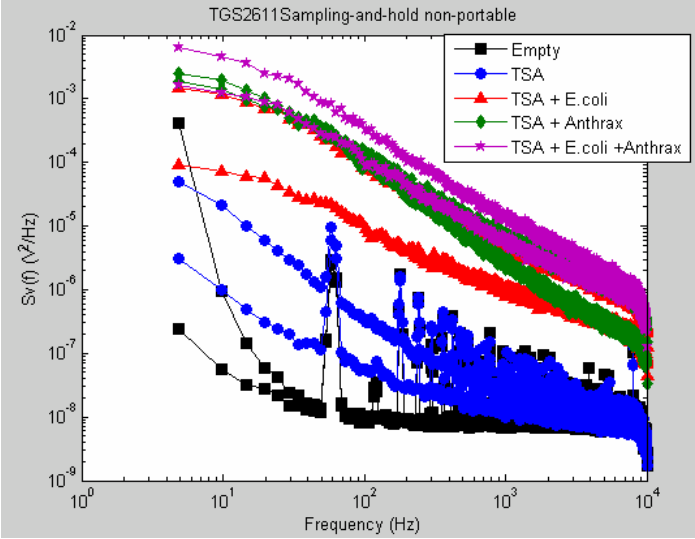

Figure 3.8 Raw power spectra of the sampling-and-hold sensor TGS2611 (non-portable device) converted by the software written by Matlab

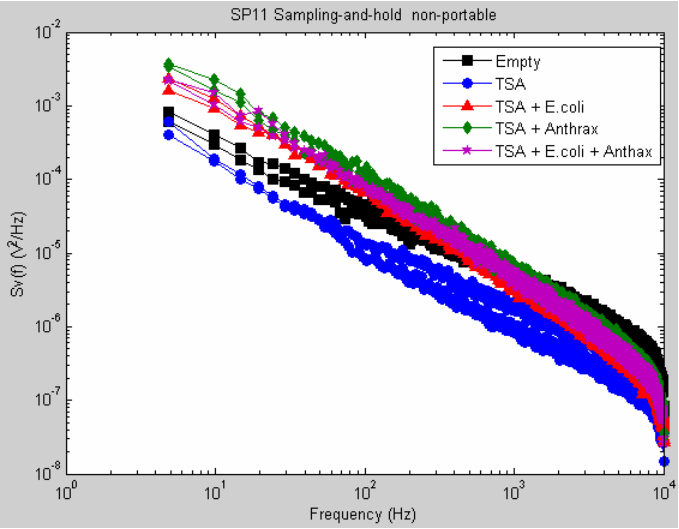

Figure 3.9 Raw power spectra of the sampling-and-hold sensor SP11 (non-portable device) converted by the software written by Matlab

Table 3.4 Summary of raw power spectra (non-portable device) converted by the software written by Matlab: + well detected/identified/repeatable; x unrecognizable/non-repeatable

Sensor	FES Mode	w/o Bacteria	empty/TSA	Bacteria Type
SP 32	Sampling-and-hold	+	+	x
TGS 2611	Sampling-and-hold	+	+	x
SP 11	Sampling-and-hold	+	+	x

3.2.2 Portable Device

As mentioned in the introduction (1.2.2.2), this device can only measure bacteria in heated mode. The raw power spectra $S_r(\Omega^2 / Hz)$ of portable device of two sensors SP11 and TGS 2611 in the heated mode are as shown in Figures 3.10 and 3.11. The amplitudes of the power spectra are amplified by gain square ($10^2 = 100$). The results are the same as these of non-portable device. The spectra of SP 11 in heated mode can be clearly divided by two groups: Empty/TSA and TSA with bacteria. The spectra of TGS 2611 in heated mode cannot be clearly differentiated due to large variations and overlaps of the spectra. As a result summarized in Table 3.5, only SP11 in heated mode can recognize samples with or without bacteria.

The sensitivity and selectivity of the portable device compared poorly with these of the non-portable device because this portable device can be operated in heated mode only. The results of non-portable device show that the sensors in sampling-and-hold yield better sensitivity and selectivity. To improve its sensitivity and selectivity, the portable device has to have a sampling-and-hold mode by using voltage source or smaller current source.

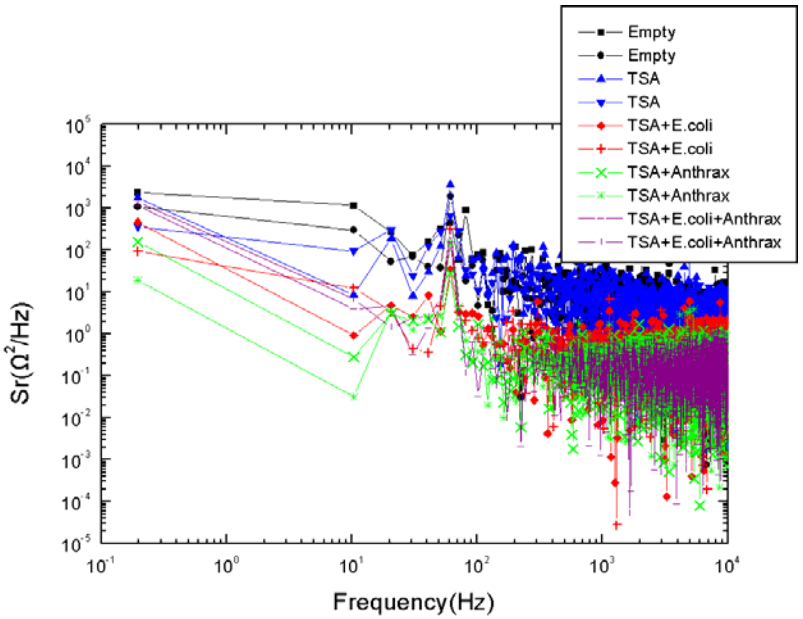

Figure 3.10 Raw power spectra of sensor SP11 in heated mode (portable device)

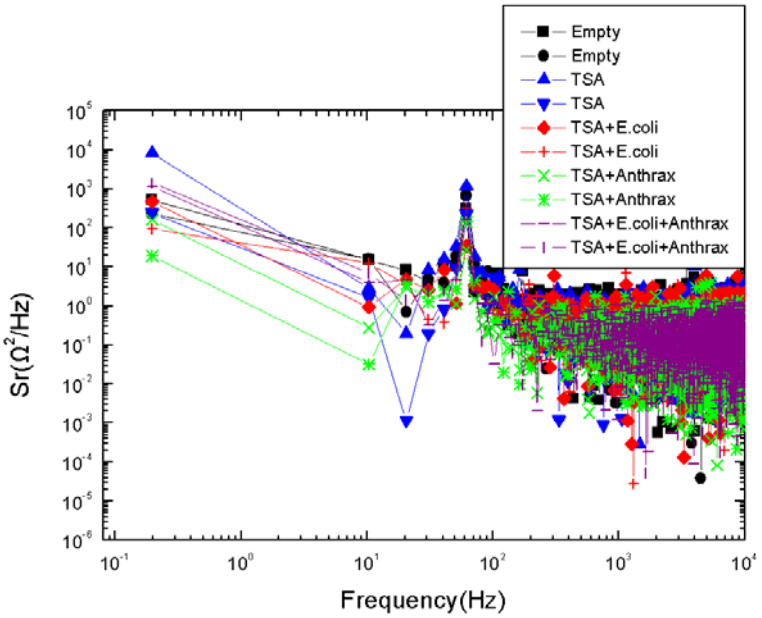

Figure 3.11 Raw power spectra of sensor TGS2611 in heated mode (portable device)

Table 3.5 Summary of raw power spectra of portable device: + well detected/identified/repeatable; x unrecognizable/non-repeatable

Sensor	FES Mode	w/o Bacteria	empty/TSA	Bacteria Type
TGS 2611	Heated	x	x	x
SP 11	Heated	+	x	x

3.3 Continuous Pattern and Binary Pattern

In this section, the following normalization of the power density spectrum of resistance fluctuations from the non-portable device (some from Section 2.2.1) was used to obtain the continuous and binary patterns:

$$\gamma(f) = f\frac{S_r(f)}{R_s^2} \quad , \tag{13}$$

where f is the frequency, $S_r(f)$ is the power density spectrum of measured resistance fluctuations, and R_s is the measured sensor resistance, and the unit of $\gamma(f)$ is 1. The $\gamma(f)$ for sensors SP32, TGS 2611, and SP11, with the tested bacterium samples, for both

the heated and sampling-and-hold sensor measurements, are given in Published Paper 3 and Section 2.2.1.1, and their amplitudes and slopes have good reproducibility.

The first step of generating a highly distinguishable pattern is used to quantify the average slopes of $\gamma(f)$ in distinct frequency ranges. The average slopes of $\gamma(f)$ are measured in six frequency bands with logarithmically equidistant widths: 100~333Hz, 0.333~1kHz, 1~3.3kHz, 3.3~10kHz, 10~33kHz, and 33~100kHz.

Let us make the following notations: α_n is the average slope in each frequency sub-bands (local slope) and β is the average slope over the entire measurement band (100Hz~100KHz), see Figure 3.12.

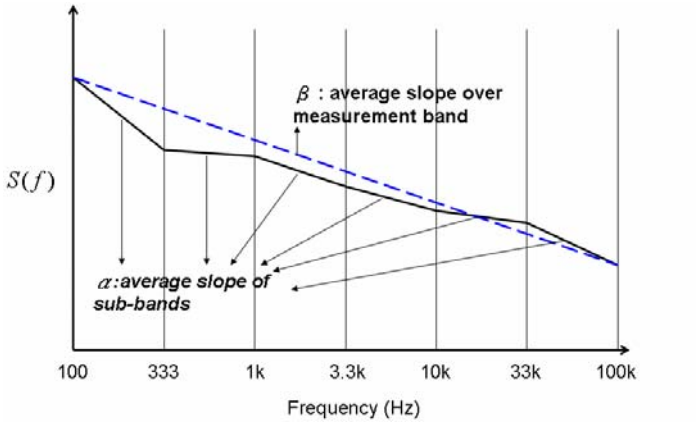

Figure 3.12 Definition of α_n and β

The deviation Δ_n of the local slope is defined for each sub-band as the difference between α_n and β in the following equation

$$\alpha_n - \beta = \Delta_n \tag{14}$$

Finally, the highly distinguishable patterns will be given by the following quantities, the sign σ_n and the normalized local deviation δ_n , respectively, see the following definitions:

$$\sigma_n = \text{signum}(\Delta_n) \tag{15}$$

$$\Delta_n = \log\left|\frac{\Delta}{\beta}\right| \tag{16}$$

Notably, the units of both σ_n and δ_n quantities are one. The quantity σ_n is a binary pattern that indicates if α is larger or smaller than β for each sub-bands of the spectrum. The advantage of the quantity σ_n is that it provides a very quick way of quantified decision if two spectral patterns are identical or not. By using a simple Boolean logic rule to evaluate these binary patterns with 6-bit values, a Boolean logic circuit can act as a pattern recognizer and distinguish each situation where the pattern is different from the others. On the other hand, δ_n is a continuum variable and offers more information when it is needed; however, the quantitative pattern recognition requires more advanced tools.

By using the σ_n histograms to represent these measurement results [5], the binary patterns can be categorized into three classes of the four available possibilities, see Figures 3.13 to 3.18. The situations inside the chamber were the *empty*, TSA, TSA+ *E. coli* or TSA+ Anthrax. *Empty* means no sample in the chamber. The criteria of the identification and reproducibility are defined by the bit error percentage. The bit errors smaller than 30% are well detected, identified, and repeatable; and the bit errors are larger than 30% are unrecognizable and non-repeatable. The experiments are repeated with numerous samples multiple times over numerous days. Most patterns obtained in the sequential experiments are similar to the patterns obtained in the first experiment. Therefore, the bit error percentage can be obtained by the patterns in the subsequent experiments compared to the pattern in the first experiment. The conclusions of using binary pattern σ_n are summarized in Table 3.6. Consequently, the simple binary pattern recognition can be used to distinguish the *bacteria* from the *no-bacteria* situations with good reproducibility with each sensor in both the *heated* and the *sampling-and-hold* working modes except the heated sensor TGS 2611. Only the binary pattern of SP32 in sampling-and-hold mode can differentiate samples with or without bacteria and TSA with perfect reproducibility except the 6^{th} bit of the empty condition.

Figures 3.19 to 3.24 show the plots of the δ_n continuum patterns for all the different cases. The repeatability of all the continuum patterns is poor for the large variations in the sequential experiments. Besides, the continuum patterns are far more complicated than the binary patterns and advanced pattern recognitions are needed to

analyze them. Consequently, it is difficult for a microprocessor-free system to implement the continuum patterns.

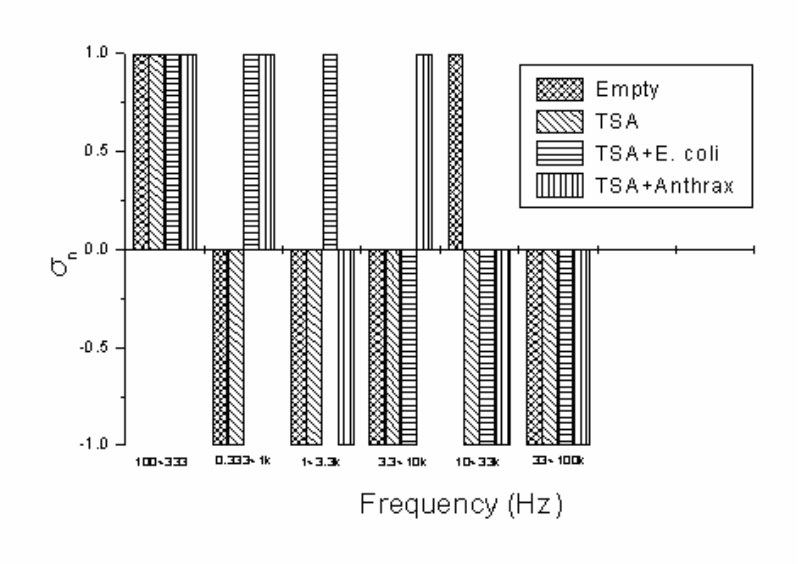

Figure 3.13 The binary pattern σ_n of the heated sensor SP32

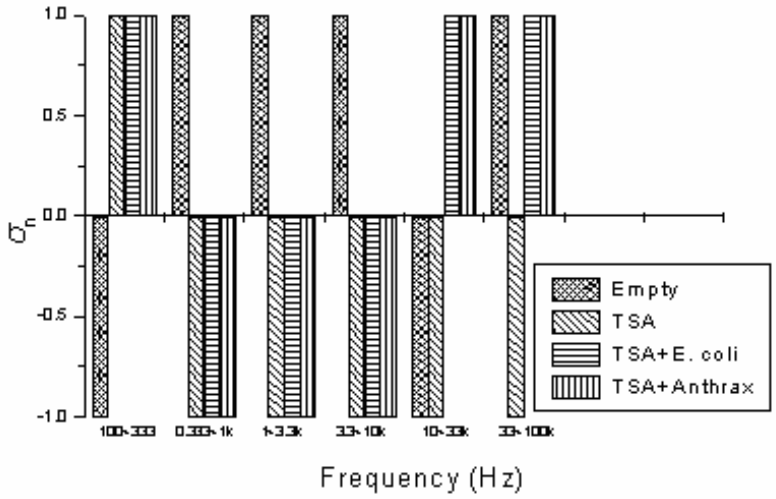

Figure 3.14 The binary pattern σ_n of the sampling-and-hold sensor SP32

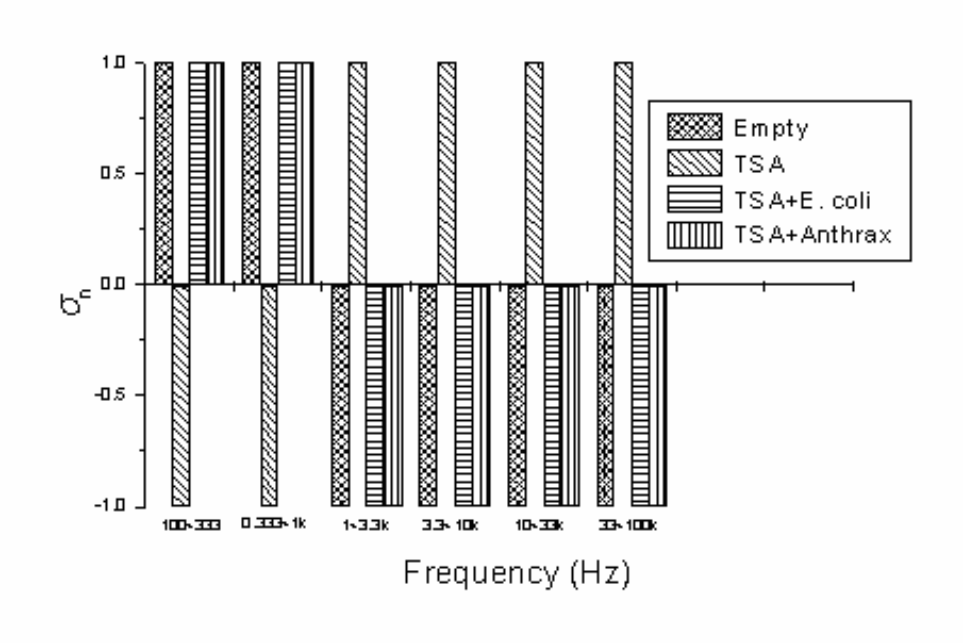

Figure 3.15 The binary pattern σ_n of the heated sensor TGS2611

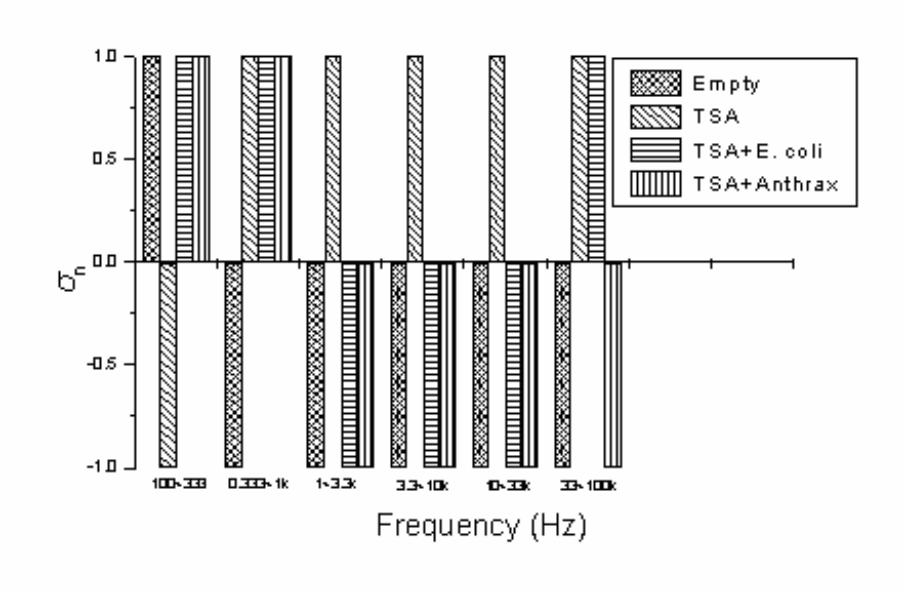

Figure 3.16 The binary pattern σ_n of the sampling-and-hold sensor TGS2611

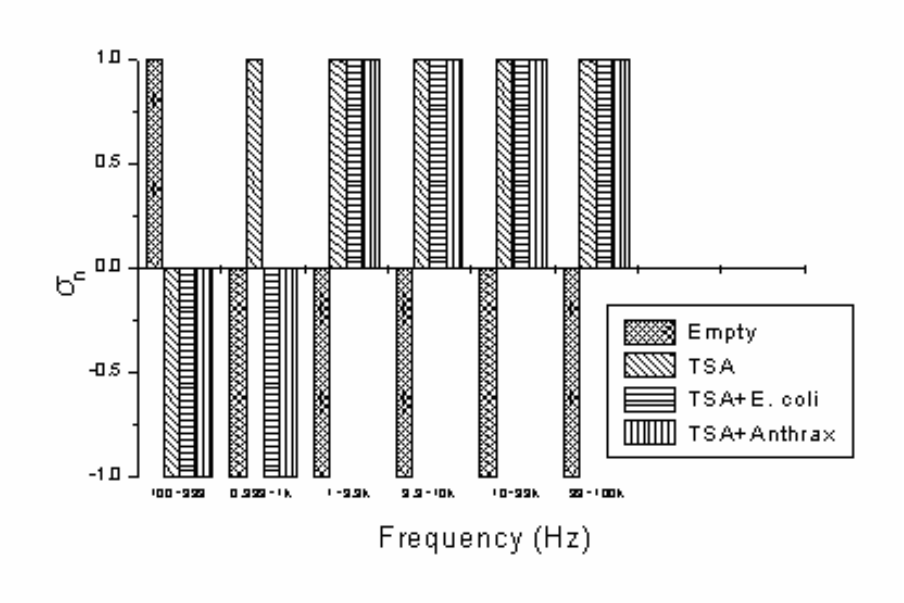

Figure 3.17 The binary pattern σ_n of the heated sensor SP11

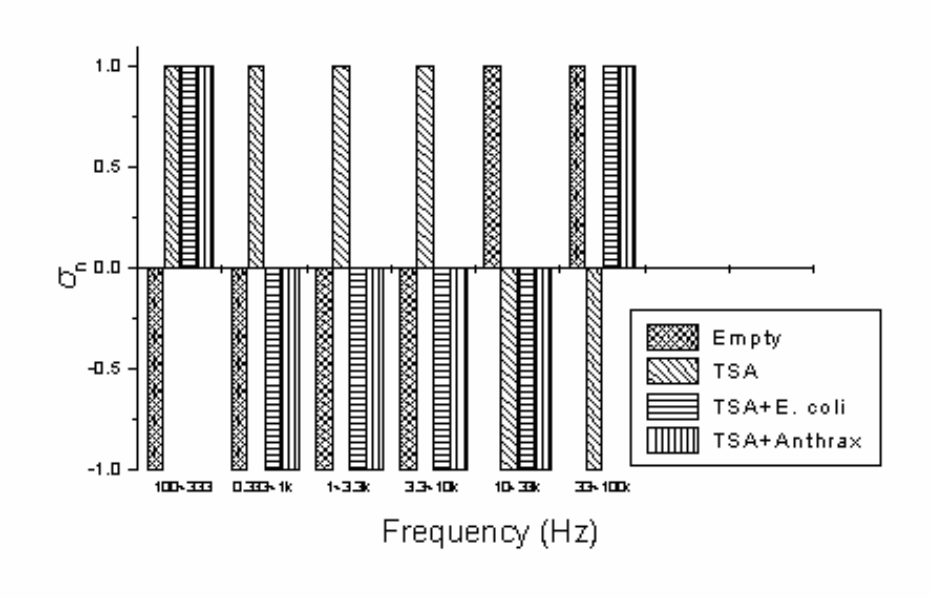

Figure 3.18 The binary pattern σ_n of the sampling-and-hold sensor SP11

Table 3.6 Summary of distinguished samples by using the binary pattern σ_n. Notations: O perfect identified/repeatable; + well identified/repeatable (<30% bit error); x unrecognizable/non-repeatable (>30% bit error)

Sensor	FES Mode	w/o Bacteria	empty/TSA	Bacteria Type
SP 32	Heated	+	+	x
SP 32	Sampling-and-hold	O	O	x
TGS 2611	Heated	x	x	x
TGS 2611	Sampling-and-hold	+	x	x
SP 11	Heated	+	x	x
SP 11	Sampling-and-hold	+	+	x

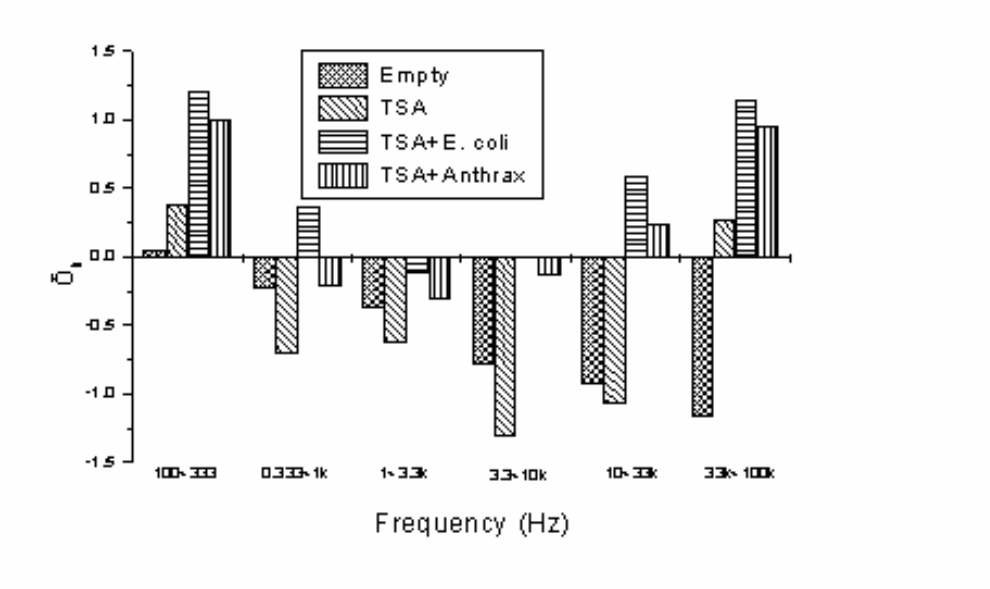

Figure 3.19 The continuum pattern δ_n of the heated sensor SP32

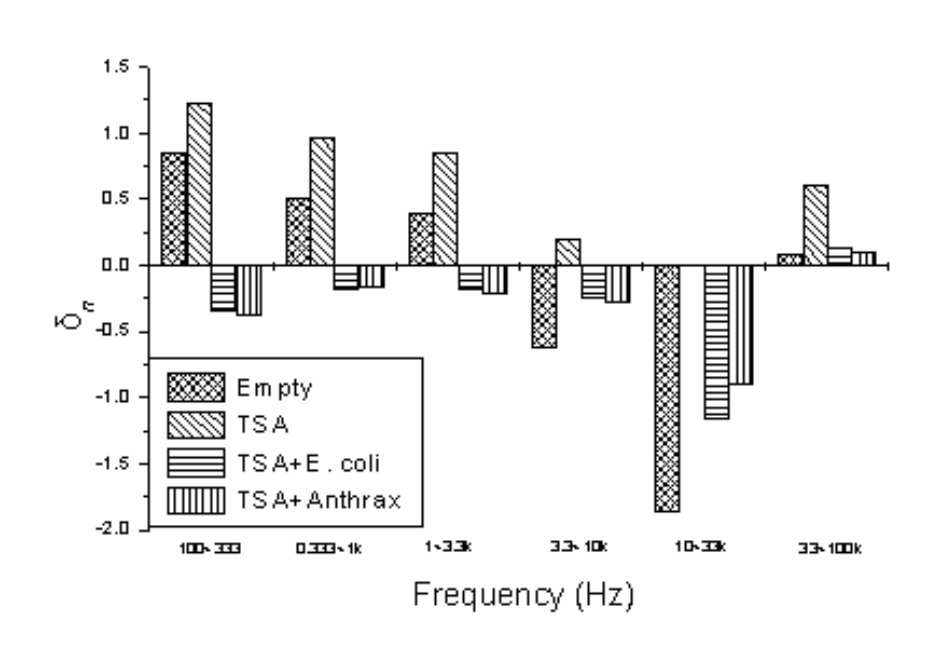

Figure 3.20 The continuum pattern δ_n of the sampling-and-hold sensor SP32

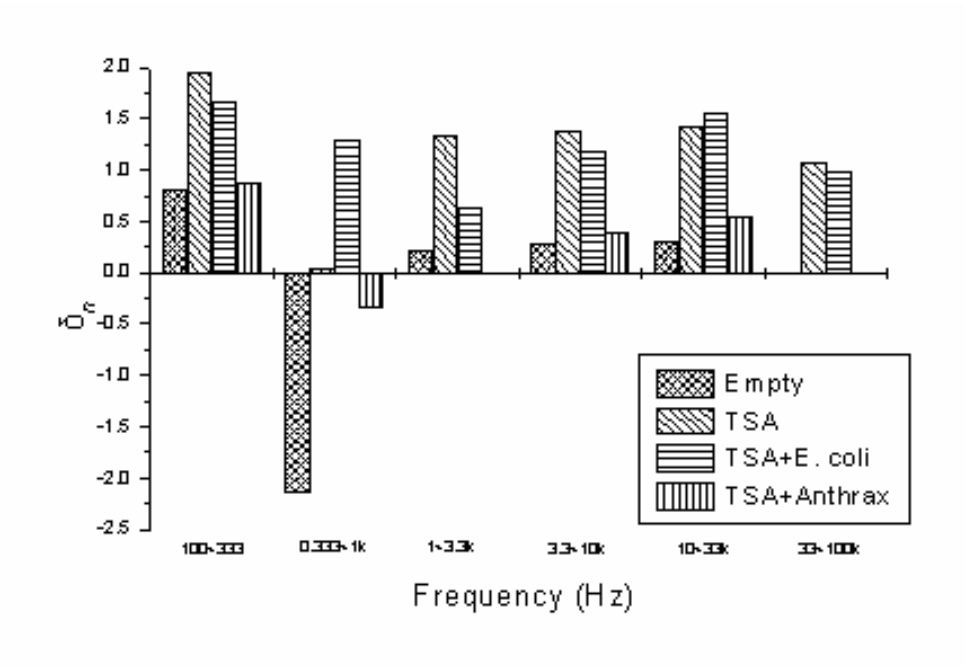

Figure 3.21 The continuum pattern δ_n of the heated sensor TGS2611

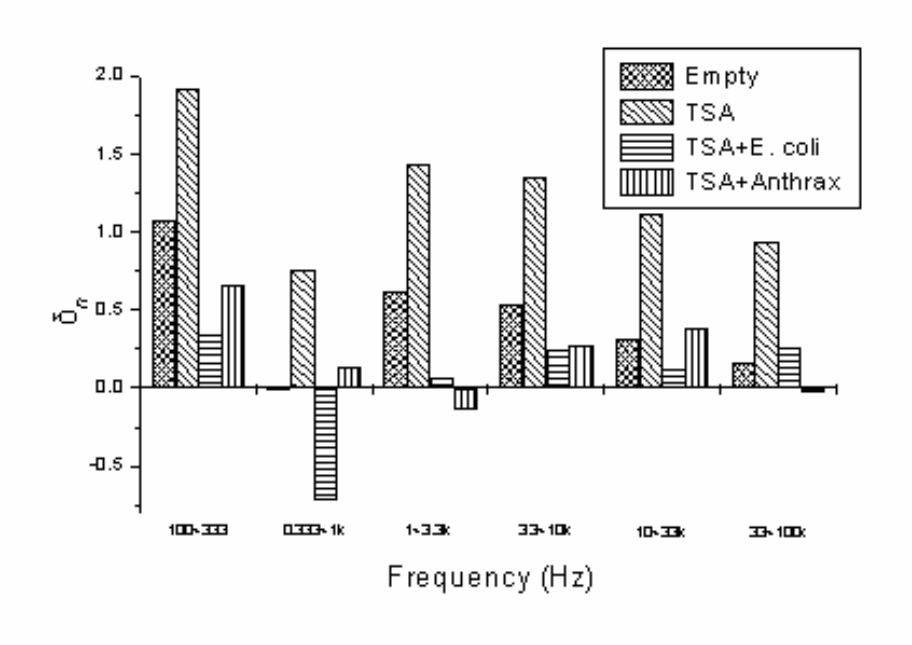

Figure 3.22 The continuum pattern δ_n of the sampling-and-hold sensor TGS2611

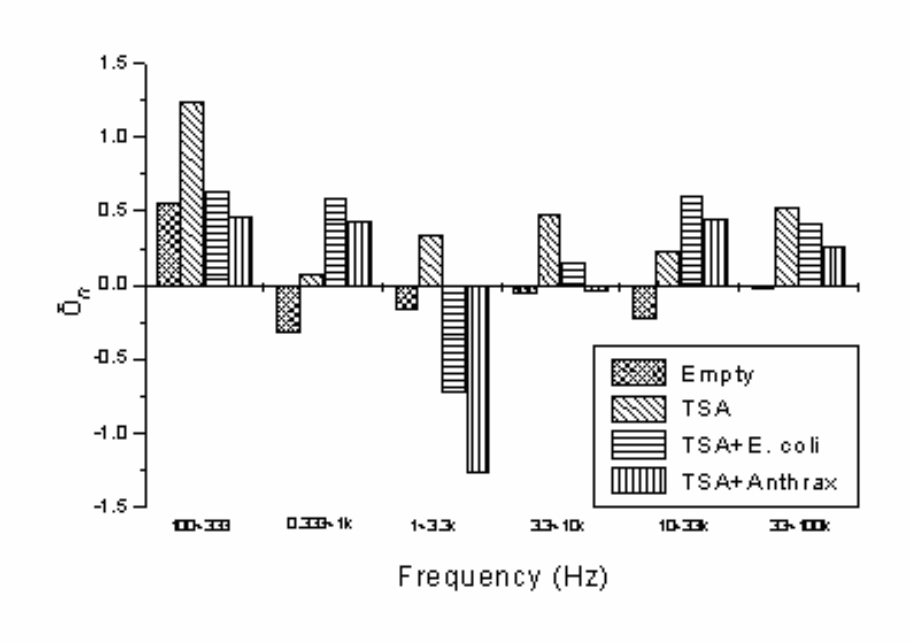

Figure 3.23 The continuum pattern δ_n of the heated sensor SP11

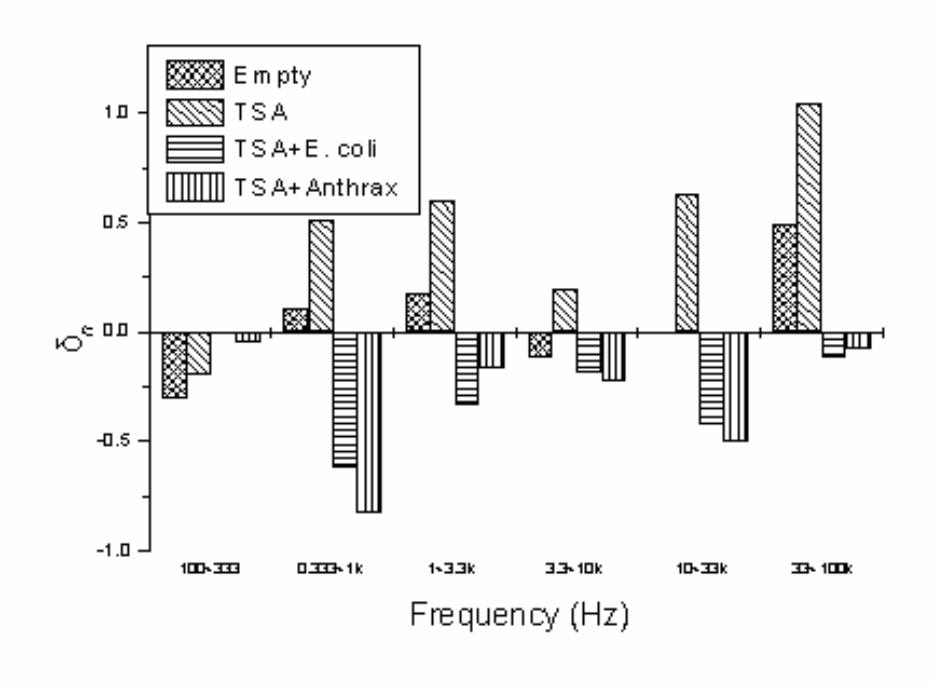

Figure 3.24 The continuum pattern δ_n of the sampling-and-hold sensor SP11

On one hand, the continuum patterns have poor reproducibility. Moreover, the continuum patterns are complicate; therefore, advanced pattern recognitions are needed to analyze the continuum patterns. On the other hand, the binary patterns can simply differentiate samples with or without bacteria and TSA in sampling and hold mode with good reproducibility except the sensor TGS2611. In addition, only the binary pattern of SP 32 in sampling-and-hold mode yielded perfect repeatability except the 6th bit of the empty condition as shown in Section 3.4. Besides, only the binary pattern can be used directly to design a microprocessor-free pattern recognition system. Therefore, only the binary pattern of SP 32 in sampling-and-hold mode can be used to design the microprocessor-free pattern recognition system in Chang et al, 2010 [6].

3.4 Characteristics of Patterns Extracted from Experiment Results

This section illustrates the characteristics of the extracted binary patterns of SP 32 in sampling-and-hold mode. For simplicity, the sub-bands were defined: 100−333 Hz for bit B1, 0.333–1 kHz for bit B2, 1−3.3 kHz for bit B3, 3.3−10 kHz for bit B4, 10−33 kHz for bit B5, and 33–100 kHz for bit B6. The binary pattern used for driving the logic circuit in Published Paper 4 was found to have the following characteristics:

(i) *Good Reproducibility*: The examples are shown in Figures 3.25 to 3.27: measurement data obtained with the independently prepared samples at different dates. However, the spectra in Figures 3.25 to 3.27 yield the identical patterns except Bit B6 of Empty condition shown in Figure 3.28. Therefore, Bit B6 of Empty condition should not be used in the Boolean logic for pattern recognition. However, the rest of the bits provide sufficient information to identify the different types of samples

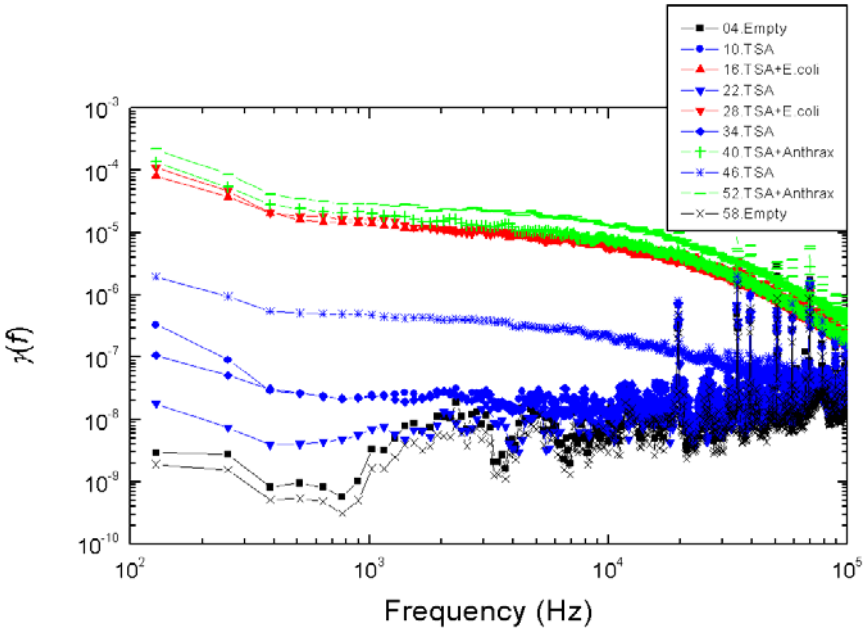

Figure 3.25 Normalized power density spectra of the resistance fluctuations of the sensor SP32 measured in the sampling-and-hold [8, 10] working mode. Each sample had one million bacteria.

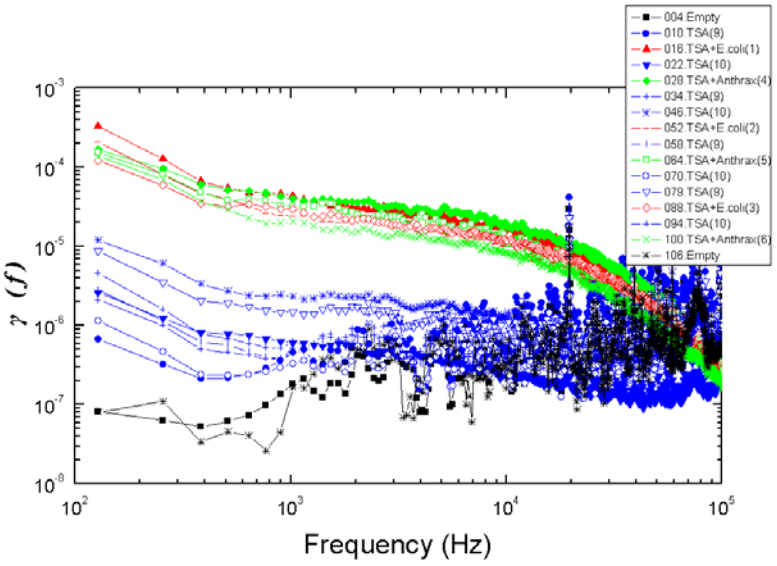

Figure 3.26 Reproducibility of the experimental data shown in Figure 3.25 with new samples

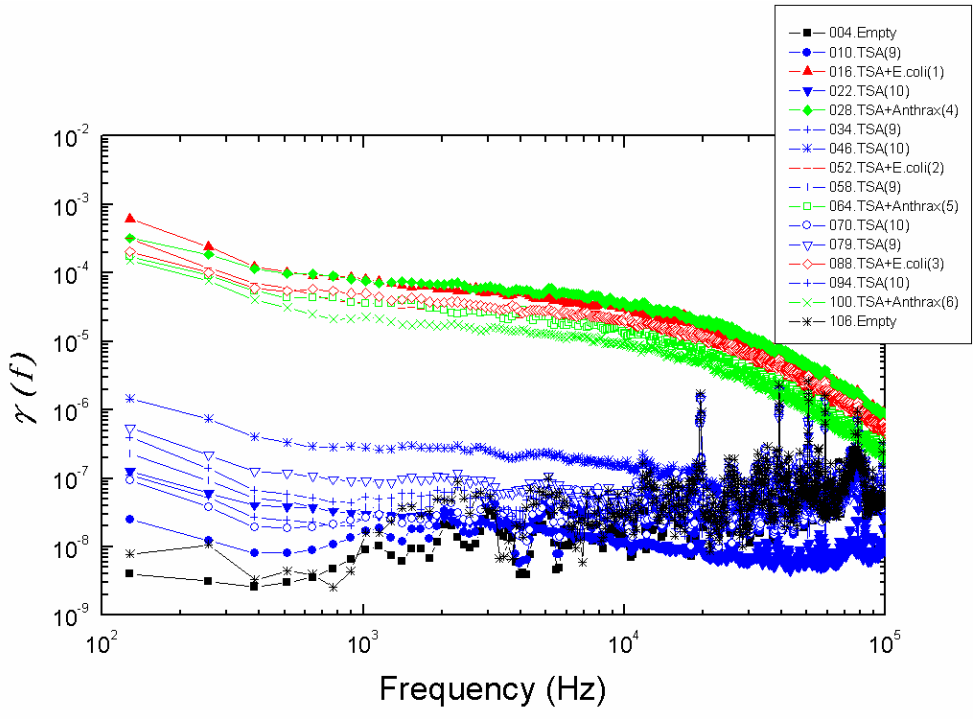

Figure 3.27 Reproducibility of the experimental data shown in Figures 3.25 to 3.26 with new samples

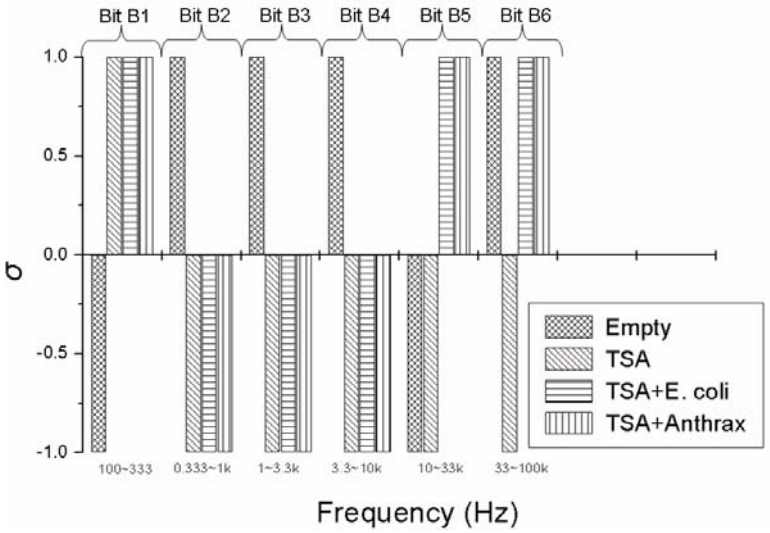

Figure 3.28 The spectra in Figures 3.25 to 3.27 yield the same 6-bits pattern except Bit B6 of Empty condition

(ii) *Inability to Differentiate between the Two Types of Bacteria*:

The applied sensor and the simple 6-bit pattern generation used for these tests were unable to differentiate between the two bacteria, while they were able to differentiate between all the other cases (empty, TSA, bacteria). This fact originates from the particular settings of the pattern generation because the differences between the spectra of the different types of bacteria could be distinguished by naked eye. However, this situation is satisfactory because the goal of this study was not to present a fully featured/optimized system but to show how much can be achieved with just the simple, ad-hoc, demo version of a 6-bits system.

(iii) *Mixture of Two Types of Bacteria*:

In addition, the following experiment was designed to observe the pattern of the mixture of two types of bacteria. Former section (i) and (ii) show that two types of bacteria have the same pattern. Therefore, the mixture of them can also be expected to have the same pattern as individual type of bacteria.

The measurement conditions were empty chamber, TSA only, TSA + *E. coli*, TSA + Anthrax, and TSA + *E. coli* + Anthrax. All the samples with bacteria are with the bacterium number of one million except for TSA + *E. coli* + Anthrax (one million E. coli + one million Anthrax). As a result, the spectra of the mixed type bacteria show the same

binary pattern as the individual type bacteria. The normalized power spectra are shown in Figure 3.29, and the binary pattern is shown in Figure 3.30.

The binary pattern in Figure 3.30 is the same as this in Figure 3.28, which can also recognize three conditions: empty, TSA, and TSA+ bacteria. Similar to the former result, all the samples with bacteria have the same binary pattern in all bits excluding the bit B5. Other bits are reliable enough to recognize the types of samples.

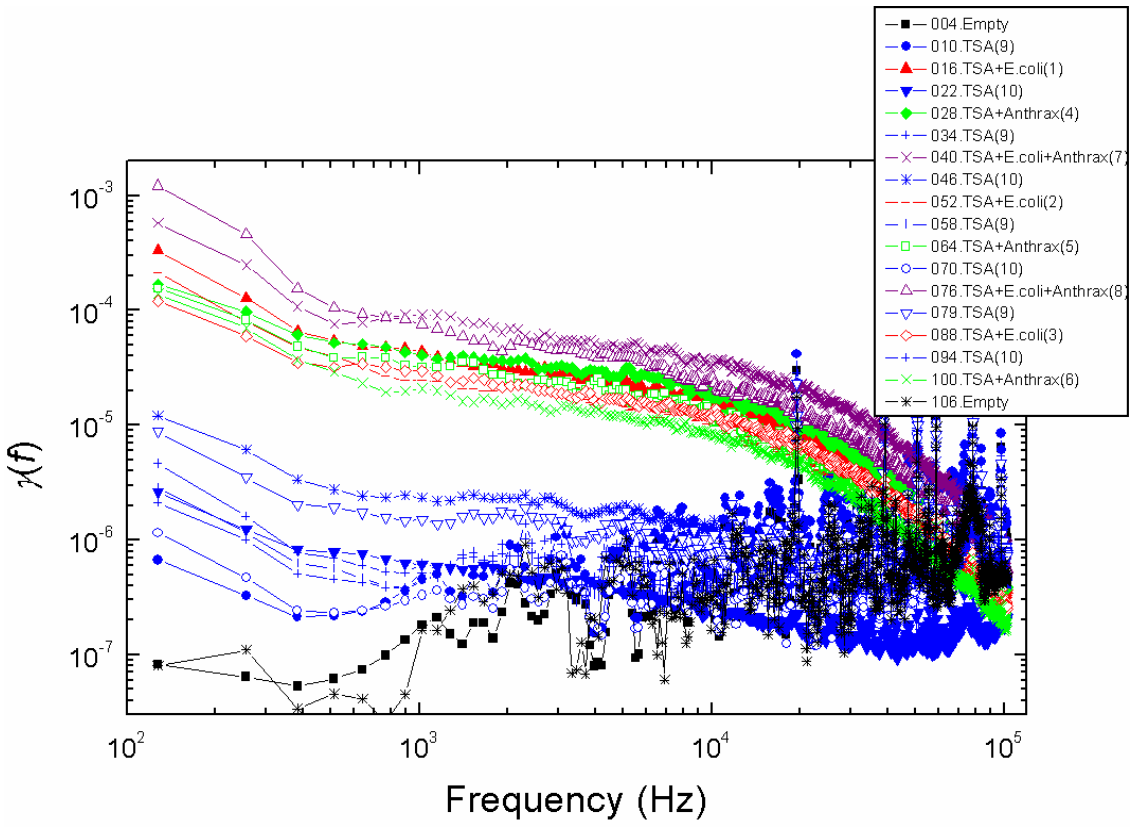

Figure 3.29 Normalized power spectra of the sampling-and-hold sensor SP32. The samples with bacteria have a population of one million except the sample with a mixture of the two bacteria with a population of one million E. coli and one million Anthrax

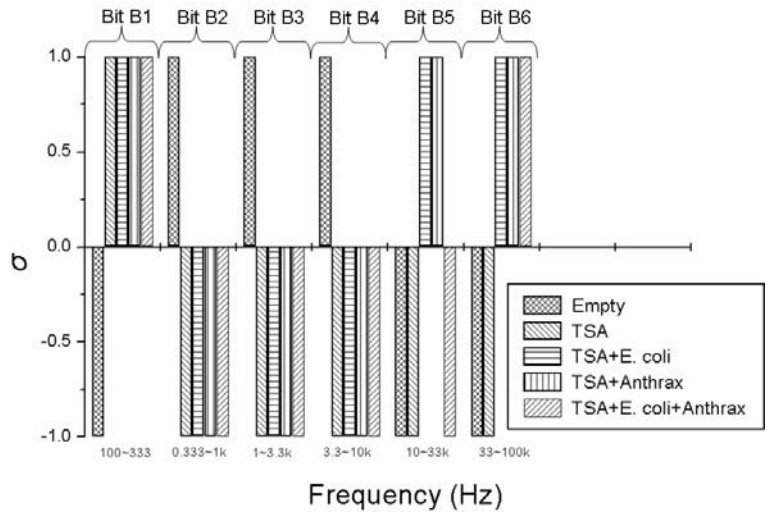

Figure 3.30 The binary pattern σ of the sampling-and-hold sensor SP32. The samples with bacteria are with the number of one million except the sample with mixture of the two bacteria with one million E coli and Anthrax

(iv) *Robustness against Variations of the Bacterium Number*:

This linear characteristic was unexpected with Taguchi sensors, which are nonlinear devices, but they could be expected with linear sensors. The linear response of nonlinear sensors against small perturbations was tested in the following.

The measurement conditions to test the impact of bacterium numbers were as follows. Six different bacterium numbers of E. coli were used: 2.5×10^4, 5×10^4, 10^5, 2.5×10^5, 5×10^5, and 10^6. The normalized power density spectra and the binary patterns are shown in Figures 2.4.7 and 2.4.8, respectively.

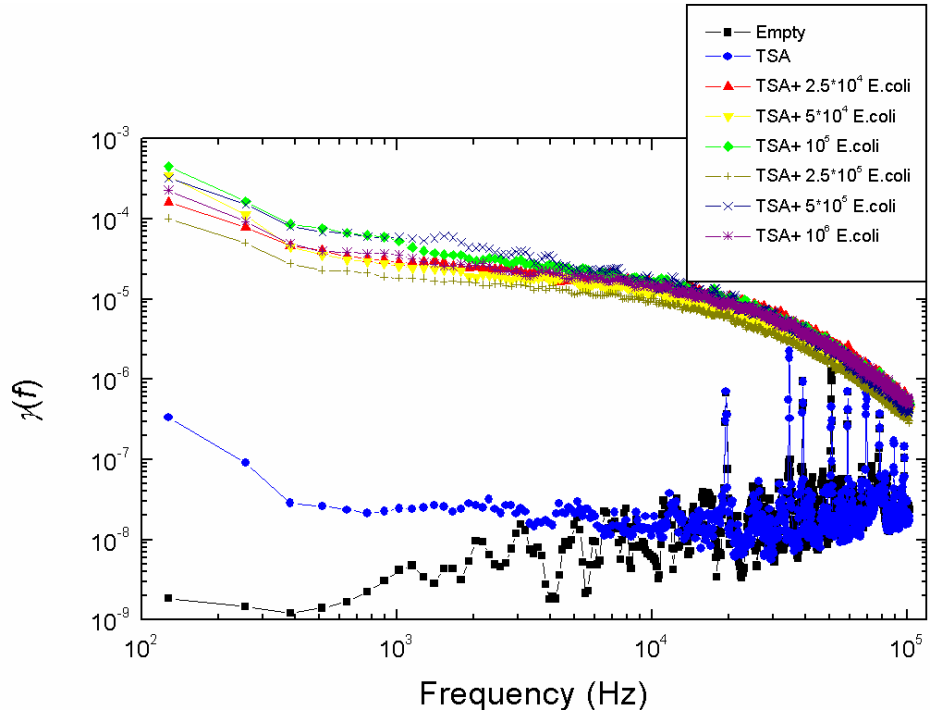

Figure 3.31 Variations of the normalized power density spectrum at different bacterium numbers

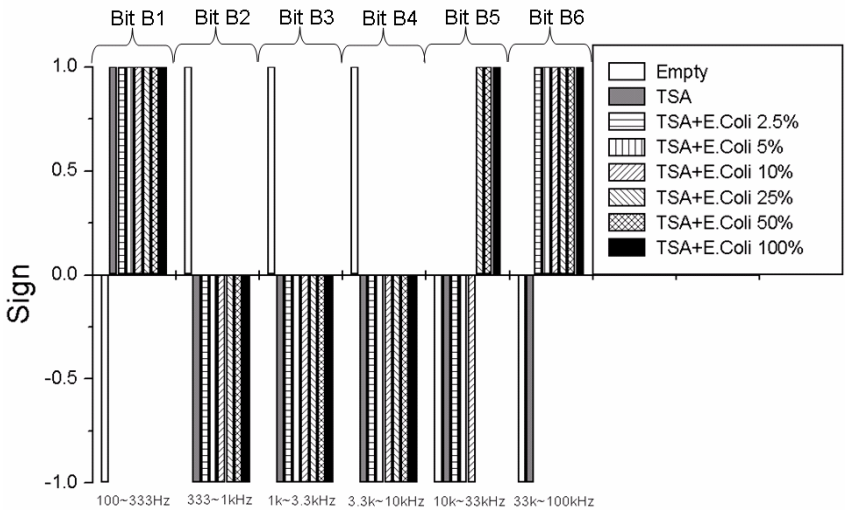

Figure 3.32 Variations of the binary pattern at different bacterium numbers. Bit B5 is not reliable therefore that bit should not be used for pattern recognition

The binary pattern in Figure 3.32 can also identify three conditions: empty, TSA, and TSA + bacteria (*E. coli*). When the bacterium number decreases from 10^6 to 2.5×10^4, the bits remained the same except bit B5 (relevant to sub-band 10 k~33 kHz). Consequently, bit B5 should not be used in the Boolean logic for pattern recognition, except perhaps as extra information about the bacterium number. However, the rest of the bits provide sufficient information to identify the different types of samples: empty, TSA, and TSA + bacteria (*E. coli*).

In Chang et al, 2010 [6], this new type of signal processing and pattern recognition can be implemented with a microprocessor-free system using building elements of analog circuitries and a few logic gates with ultra low power consumption.

4. CONCLUDING REMARKS*

This dissertation presents two kinds of sensing applications of fluctuation and noise: soil bulk density assessment and bacterium sensing.

In order to obtain the information of soil bulk density, the measurement of Vibration-Induced Conductivity Fluctuations (VICOF) was proposed. In the initial phase of study [3], the relations between the soil bulk density, wetness, salinity, and VICOF data were found through simple theory, simulations, and experiments. In the subsequent phase [4], the new methods and their theory were designed to improve the weaknesses of the initial approach, such as large data scattering due to loose contacts and two electrode resistance measurements.

The new theory was proposed to obtain the relationship between the measured signal and the electromechanical transport parameters of the soils. The new methods include the new four-electrode measurements and the new schemes. By using the four-electrode measurement with line or plane contacts cooperated with the vertical compression or the vertical vibration method, the applied force can be perpendicular to the current, and the exact value of soil resistivity can be derived directly. Besides the former advantage, the vertical compression and vibration methods can minimize the loose electrode impacts on the measurement in accuracy and reproducibility.

In the bacterium sensing study, Fluctuation-Enhanced Sensing (FES) with commercial Taguchi sensors was used to detect and identify bacteria by sensing their odor. In the initial phase of the study [5], the possibility of detecting bacteria by sensing their odor via two FES modes (Regular sensing (RS) and Sampling-and-hold (SH)) with commercial Taguchi sensors was verified.

In this study, two devices (non-portable and portable devices) and two methods of analysis (spectral data obtained by the power spectrum analyzer and spectral data converted from the time data) were used. As a result, the non-portable device in sampling-and-hold mode and the spectral data converted from time data can improve the sensitivity, selectivity and reproducibility of sensors.

Lastly, the simple method to generate continuous and binary patterns extracted from measurement data based on the spectral slopes in different frequency ranges at Fluctuation-Enhanced Sensing was proposed in Chang et al, 2010 [6]. As a result, only the binary pattern of sensor SP 32 in sampling-and-hold mode performs perfect

repeatability. This new type of signal processing and binary pattern recognition can be implemented with a microprocessor-free system using building elements of analog circuitries and a few logic gates with ultra low power consumption.

REFERENCES

[1] J. W. Wu, H. C. Chang, and T. Wang, Oxide soft breakdown effects on drain current flicker noise in ultra-thin oxide CMOS devices, SSDM Negoya, Japan (2002) 698–699.

[2] J. W. Wu, C. C. Cheng, K. L. Chiu, J.C. Guo, W. Y. Lien, C.S. Chang, G. W. Huang, and T. Wang, Pocket implantation effect on drain current flicker noise in analog nMOSFET devices, IEEE Transactions on Electron Devices 51(8) (2004)1262-1266.

[3] A.Sz. Kishné, C.L.S. Morgan, H.C. Chang, and L.B. Kish, Vibration-induced conductivity fluctuation measurement for soil bulk density analysis, Fluctuation and Noise Letters 7(4) (2007) L473-L481.

[4] H.C. Chang, L.B. Kish, A.Sz. Kishné, C.L.S. Morgan, Theory and techniques for vibration-induced conductivity fluctuation testing of soils, Fluctuation and Noise Letters 8(2) (2008) L125-L140.

[5] H.C. Chang; L.B. Kish; M.D. King; C. Kwan. Fluctuation-enhanced sensing of bacterium odors. Sens. Actuators, B 142 (2009) 429-434.

[6] H.C. Chang; L.B. Kish; M.D. King; C. Kwan. Binary fingerprints at fluctuation-enhanced sensing Sensors, 10(1) (2010) 361-373.

[7] R.B. Grossman, and T.G. Reinch, Bulk density and linear extensibility, Chapter 2.1. Methods of Soil Analysis. Part 4, Physical Methods, SSSA Book Series 5, 2002, 201-228.

[8] L.C. Timm, L.F. Pires, K. Reichardt, R., R. Rovetti, J.C.M. Oliveira and O.O.S. Bacchi, Soil bulk density evaluation by conventional and nuclear methods, Australian J. of Soil Res. 43 (2005) 97-103.

[9] Yu, X. and V.P. Drnevich, Soil water content and dry density by Time Domain Reflectometry, J. Geotech. And Geoenvir. Engrg. 130 (9) (2004) 922-934.

[10] L.B. Kish, C.L.S. Morgan and A.Sz. Kishné, Vibration-induced conductivity fluctuation (VICOF) testing of soils, Fluctuation and Noise Letter 6(4) (2006) L359-L365.

[11] A.Sz. Kishné, C.L.S. Morgan and L.B. Kish, Measuring soil bulk density by using vibration-induced conductivity fluctuation, 18th World Congress of Soil Science, Philadelphia, PA, USA, Abstracts, (2006) 282.

[12] S. Chanda, Implications of aerobiology in respiratory allergy, Ann. Agric. Environ.Med. 3 (1996) 157–164.

[13] J. Lacey, J. Dutkiewicz, Bioaerosols and occupational lung disease, J. Aerosol. Sci.25 (8) (1994) 1371–1404.

[14] L.B. Kish, R. Vajtai, C.G. Granqvist, Unsolved problems of noise and fluctuations, in: Proceedings of 2nd International Conference on Unsolved Problems of Noise (UPoN‘99), Adelaide, Australia, 1999, American Institute of Physics, Melville, NY(2000), p. 463.

[15] J.W. Gardner, P.N. Bartlett, ElectronicNoses: Principles and Applications, Oxford University Press, Oxford, 1999.

[16] L.B. Kish, J. Smulko, P. Heszler, C.G. Granqvist, On the sensitivity, selectivity, sensory information and optimal size of resistive chemical sensors, invited paper, Nanotechnol. Percept. 3 (2007) 43–52.

[17] G. Schmera, L.B. Kish, Fluctuation enhanced chemical sensing by surface acoustic wave devices, Fluctuation Noise Lett. 2 (2002) L117–L123.

[18] G. Schmera, L.B. Kish, Surface diffusion enhanced chemical sensing by surface acoustic waves, Sens. Actuators, B 93 (2003) 159–163.

[19] J.L. Solis, G. Seeton, Y. Li, L.B. Kish, Fluctuation-enhanced sensing with commercial gas sensors, Sens. Transducers Mag. 38 (2003) 59–66.

[20] J. Smulko, J. Ederth, L.B. Kish, P. Heszler, C.G. Granqvist, Higher-order spectra in nanoparticle gas sensors, Fluctuation Noise Lett. 4 (2004) L597–L603.

[21] J.M. Smulko, L.B. Kish, Higher-order statistics for fluctuation-enhanced gassensing, Sens. Mater. 16 (2004) 291–299.

[22] J.M. Smulko, J. Ederth, Y. Li, L.B. Kish, M.K. Kennedy, F.E. Kruis, Gas-sensing by thermoelectric voltage fluctuations in SnO2 nanoparticle films, Sens. Actuators, B 106/2 (2005) 708–712.

[23] L.B. Kish, Y. Li, J.L. Solis, W.H. Marlow, R. Vajtai, C.G. Granqvist, V. Lantto, J.M. Smulko, G. Schmera, Detecting harmful gases using fluctuation-enhanced sensing, IEEE Sens. J. 5 (2005) 671–676.

[24] J.L. Solis, G.E. Seeton, Y. Li, L.B. Kish, Fluctuation-enhancedmultiple-gas sensing, IEEE Sens. J. 5 (2005) 1338–1345.

[25] J. Ederth, J.M. Smulko, L.B. Kish, P. Heszler, C.G. Granqvist, Comparison of classical and fluctuation-enhanced gas sensing with PdxWO3 nanoparticle films, Sens. Actuators, B 113 (2006) 310–315.

[26] S. Gomri, J.L. Seguin, K. Aguir,Modelling on oxygen chemisorption induced noise in metallic oxide gas sensors, Sens. Actuators, B 107 (2005) 722–729.

[27] S. Gomri, J.L. Seguin, J. Guerin, K. Aguir, Adsorption–desorption noise in gas sensors: modelling using Langmuir and Wolkenstein models for adsorption, Sens. Actuators, B 114 (2006) 451–459.

[28] Ch. Kwan, G. Schmera, J. Smulko, L.B. Kish, P. Heszler, C.G. Granqvist, Advanced agent identification at fluctuation-enhanced sensing, IEEE Sens. J. 8 (2008) 706–713.

[29] G. Schmera, Ch. Kwan, P. Ajayan, R. Vajtai, L.B. Kish, Fluctuation-enhanced sensing: status and perspectives, IEEE Sens. J. 8 (2008) 714–719.

[30] L.B. Kish, R. Vajtai, C.G. Granqvist, Unsolved problems of noise and fluctuations, in: Proceedings of 2nd International Conference on Unsolved Problems of Noise (UPoN‘99), Adelaide, Australia, 1999, American Institute of Physics, Melville, NY, 2000, p. 463.

[31] L.B. Kish, R. Vajtai, C.G. Granqvist, Extracting information from noise spectra of chemical sensors: single sensor electronic noses and tongues, Sens. Actuators, B 71 (2000) 55–59.

[32] L.B. Kish, C.G. Granqvist, R. Vajtai, Sampling-and-Hold Chemical Sensing by Noise Measurements for Electronic Nose Applications, Swedish patent (1999) Ser. No.: 990409-5.

[33] J.L. Solis, L.B. Kish, R. Vajtai, C.G. Granqvist, J. Olsson, J. Schnurer, V. Lantto, Nanocrystalline tungsten oxide thick films with high sensitivity to H2S at room temperature, Sens. Actuators, B 77 (2001) 316–321.

[34] J. Smulko, C.G. Granqvist, L.B. Kish, On the statistical analysis of noise in chemical sensors and its application for sensing, Fluctuation Noise Lett. 1 (2001) L147–L153.

[35] S. Nakata, S. Akakabe, M. Nakasuji, K. Yoshikawa, Gas sensing based on a nonlinear response: discrimination between hydrocarbons and quantification of individual components in a gas mixture, Anal. Chem. 68 (1996) 2067–2072.

[36] A. Heiling, N. Barsan, U.Weimar, M. Schweizer-Berberich, J.K. Gardner,W. Gopel, Gas identification by modulating temperatures of SnO2-based thick films sensors, Sens. Actuators, B 43 (1997) 45–51.

[37] J.W. Gardner, P.N. Bartlett, Electronic Noses: Principles and Applications, Oxford University Press, Oxford, 1999.

[38] G.E. Searle, J.W. Gardner, M.J. Chappell, K.R. Godfrey, M.J. Chapman, System Identification of electronic nose data from cyanobacteria experiments, IEEE Sensors J. 2 (2002) 218–229.

[39] S. Ampuero, J.O. Bosset, The electronic nose applied to dairy products: a review, Sens. Actuators, B 94 (2003) 1–12.

[40] K.C. Persaud, Medical applications of odor-sensing devices, New Technol. 4 (2005) 50–56.

[41] F.N. Hooge, T.G.M. Kleinpenning, L.K.J. Vandamme, Experimental studies on 1/f noise, Rep. Prog. Phys. 44 (1981) 479–532.

[42] M.B.Weissman, 1/f noise and other slow, nonexponential kinetics in condensed matter, Rev. Mod. Phys. 60 (1988) 537–571.

APPENDIX

Published Paper 1: Vibration-Induced Conductivity Fluctuation Measurement for Soil Bulk Density Analysis

The measurement of Vibration-Induced Conductivity Fluctuations (VICOF) was proposed to obtain the information about the bulk density and other parameters of soils. The measurement setup, based on mechano-electrical-transport method, can measure soil porosity and bulk density non-destructively, which is demonstrated on clay and fine sand soils using blade and cylindrical electrodes.

This paper [3] demonstrates the methodology and measurement setup and results of VICOF experiments and obtained the following conclusions. On one hand, the blade electrodes have better performance than the cylindrical electrode, because the blade electrodes have less set-up noise in the measurement of normalized vibration-induce conductivity (VICOF) On the other hand, the theory, computer simulations and measurement results in this paper elucidated that the ratio of transversal/longitudinal normalized VICOF is independent of moisture and salinity affects. Therefore, the moisture and salinity of soil samples do not affect the normalized VICOF signals.

However, these experimental data have large scattering due to the loose and heavy contacts Therefore, the new methods and schemes were proposed in Chang et al, 2008 [4] to improve the effect of the poor contacts

Published Paper 2: Theory and Techniques for Vibration-Induced Conductivity Fluctuation Testing of Soils

This paper [4] presents the new methods, arrangements, and schemes of VICOF. The new VICOF model of electromechanical response illustrates the relationship between applied vibrations, stress and strain, resistance and resistance variation. Based on the model, the new arrangements and schemes of VICOF for both the laboratory and field measurements were invented.

The new arrangements are the four-electrode measurement with line or plate contacts; and the new schemes have vertical vibration and compression VICOF in the transversal directions of the current. The new arrangements and schemes provide two advantages. The applied force can be perpendicular to the current, and the exact value of the soil resistivity can be derived directly. Also, the vertical vibration and compression methods can minimize the loose electrode impacts on the measurement in accuracy and reproducibility.

Published Paper 3: Fluctuation-Enhanced Sensing of Bacterium Odors

This paper [5] reveals the possibility of detecting and identifying bacteria by sensing their odor via of Fluctuation-Enhanced Sensing (FES) with commercial Taguchi sensors. Two FES modes were used in this study: the heated and the sampling-and-hold working modes.

The simplest method and the measurement and analysis of power density spectra were used. The fluctuations of the electrical resistance of these sensors working in two FES modes during exposure to different bacterial odors, Escherichia Coli and Anthrax *Bacillus subtilis*, were measured and analyzed. The results indicate that the Taguchi sensors used in these fluctuation-enhanced modes can be effective tools of bacterium detection and identification even when they are utilizing only the power density spectrum of the stochastic sensor signal.

The advanced stochastic signal analysis at the time data level [27] is a powerful tool and has potentials to further enhance the detectability of this type of sensing and will be the subject of subsequent studies.

Published Paper 4: Binary Fingerprints at Fluctuation-Enhanced Sensing

This paper [6] presents the method to generate and test the highly distinguishable and robust types of the binary patterns from the power density spectra based on the spectral slopes in different frequency ranges obtained at Fluctuation-Enhanced Sensing of bacterial odors. These binary patterns can be considered as the binary "fingerprints" of odors. These findings were demonstrated by single-sensor (commercial semiconducting metal oxide (Taguchi) sensor) experiments recognizing the situations of empty chamber, Tryptic Soy Agar (TSA) medium, or TSA with bacteria with 100% success rate and 0% false alarm rate. A microprocessor-free pattern recognizer was also designed to generate these binary patterns, including analog circuitries of ultra-low power consumption and a Boolean logic based pattern recognizer with negligible power consumption.

VITA

Hung-Chih Chang was born in Taipei, Taiwan. He received the B.S. degree in electrical engineering from National Central University, Taoyuan, Taiwan in 2000, and the M.S. degree in electrical engineering from National Chiao Tung University, Hsinchu, Taiwan, in 2002. During 2005 and 2006, he worked at the Taiwan Semiconductor Manufacture Company (TSMC) in Hsinchu, Taiwan where he was involved in 90/80/65nm MOS device processes and characterizations. He graduated with his Ph.D. in 2010 at the Department of Electrical and Computer Engineering at Texas A&M University, College Station. His main research interests include noise and fluctuation, MOSFET modeling, VICOF, chemical and biological sensors.

Mr. Chang's email is hungchih65@gmail.com.

Department of Electrical and Computer Engineering,

Texas A&M University,

214 Zachry Engineering Center,

TAMU 3128

College Station, Texas 77843-3128